Pergamon

Geochimica et Cosmochimica Acta, Vol. 66, No. 16, pp. 2823–2839, 2002

0016-7037/02 $22.00 + .00

PII S0016-7037(02)00878-5

Immobilization of strontium during iron biomineralization coupled to dissimilatory hydrous ferric oxide reduction

ERIC E. RODEN,[1,*] MICHAEL R. LEONARDO[1] and F. GRANT FERRIS[2]

[1]Department of Biological Sciences, The University of Alabama, Tuscaloosa, AL 35487-0206, USA
[2]Department of Geology, University of Toronto, Toronto, Canada, M5S 3B1

(*Received April* 17, 2001; *accepted in revised form February* 27, 2002)

Abstract—The potential for incorporation of strontium (Sr) into biogenic Fe(II)-bearing minerals formed during microbial reduction of synthetic hydrous ferric oxide (HFO) was investigated in circumneutral bicarbonate-buffered medium containing $SrCl_2$ at concentrations of 10 μM, 100 μM, or 1.0 mM. $CaCl_2$ (10 mM) was added to some experiments to simulate a Ca-rich groundwater. In Ca-free systems, 89 to 100% of total Sr was captured in solid-phase compounds formed during reduction of 30 to 40 mmol Fe(III) L^{-1} over a 1-month period. A smaller fraction of total Sr (25 to 34%) was incorporated into the solid phase in cultures amended with 10 mM $CaCl_2$. X-ray diffraction identified siderite and ferroan ankerite as major end products of HFO reduction in Ca-free and Ca-amended cultures, respectively. Scanning electron microscopy–energy dispersive x-ray spectroscopy revealed the presence of Sr associated with carbonate phases. Selective extraction of HFO reduction end products indicated that 46 to 100% of the solid-phase Sr was associated with carbonates. The sequestration of Sr into carbonate phases in the Ca-free systems occurred systematically according to a heterogeneous (Doerner-Hoskins) partition coefficient ($D_{D\text{-}H}$) of 1.81 ± 0.15. This $D_{D\text{-}H}$ value was 2 to 10 times higher than values determined for incorporation of Sr (10 μM) into $FeCO_3$(s) precipitated abiotically at rates comparable to or greater than rates observed during HFO reduction, and fivefold higher than theoretical partition coefficients for equilibrium $Fe(Sr)CO_3$ solid solution formation. Surface complexation and entrapment of Sr by rapidly growing siderite crystals (and possibly other biogenic Fe(II) solids) provides an explanation for the intensive scavenging of Sr in the Ca-free systems. The results of abiotic siderite precipitation experiments in the presence and absence of excess Ca indicate that substitution of Ca for Sr at foreign element incorporation sites (mass action effect) on growing $FeCO_3$(s) surfaces can account for the inhibition of Sr incorporation into the siderite component of ankerite formed in the Ca-amended HFO reduction experiments. Likewise, substitution of Fe(II) for Sr may explain the absence of major Sr partitioning into the calcite component of ankerite. The findings indicate that under appropriate conditions, sequestration of metals in siderite produced during bacterial Fe(III) oxide reduction may provide a mechanism for retarding the migration of Sr and other divalent metal contaminants in anaerobic, carbonate-rich sedimentary environments.

1. INTRODUCTION

The transport and fate of trace metals and metal-radionuclide contaminants in subsurface environments is controlled by coupled physical, chemical, and microbiological processes (Hunter et al., 1998; Salvage and Yeh, 1998; Tebes-Stevens et al., 1998). Microbial metabolism can cause both dissolution and precipitation of inorganic mineral phases, primarily through redox reactions associated with organic matter oxidation (Lovley and Chapelle, 1995). Such microbially catalyzed redox reactions have the potential to strongly influence the fate of metals and radionuclides in the subsurface (Davis et al., 1993; Fish, 1993).

Microbial Fe(III) oxide reduction is a dominant microbial redox process in many anaerobic subsurface environments (Lovley, 1991). Microbial Fe(III) oxide reduction can exert wide-ranging and potentially competing impacts on metal-radionuclide contaminant mobility in subsurface sediments. Trace and contaminant metals adsorbed to Fe(III) oxides are prone to release during reductive oxide dissolution by Fe(III)-reducing bacteria (Lovley, 1991, and citations therein). However, the same process generates inorganic carbon (IC) and alkalinity, which can create conditions favorable for metal-carbonate mineral precipitation (Coleman et al., 1993). The latter effect is illustrated by the following reaction, in which a unit of organic carbon (CH_2O) is oxidized with the reduction of amorphous Fe(III) oxide, resulting in the production of bicarbonate and hydroxyl alkalinity:

$$4Fe(OH)_3 + CH_2O = 4Fe^{2+} + HCO_3^- + 7OH^- + 3H_2O. \quad (1)$$

A rise in pH and precipitation of $FeCO_3$(s) (siderite) is known to occur in bicarbonate-buffered medium in which dissimilatory Fe(III) oxide reduction is active (Roden and Lovley, 1993a; Mortimer and Coleman, 1997; Fredrickson et al., 1998). In addition, accumulation of siderite and other carbonate minerals (e.g., calcite) in a variety of surface and subsurface sediments has been attributed at least in part to microbial Fe(III) oxide reduction (Postma, 1977, 1981, 1982; Gautier, 1982; Pye, 1984; Aller et al., 1986; Baedecker et al., 1992; Saunders and Swann, 1992; Coleman, 1993; Mckinley et al., 1997).

Carbonate minerals are seldom present in nature as pure solid phases; most contain significant quantities of metal cation

* Author to whom correspondence should be addressed (eroden@bsc.as.ua.edu).

impurities in their structure (Stumm and Morgan, 1996). The incorporation of foreign cations into mineral precipitates is thought to proceed via adsorption and surface precipitation, leading to solid solution end products (Sposito, 1984). Because the solubility of a trace metal constituent can be greatly reduced when it becomes a minor component of a solid solution phase, partitioning into carbonate phases plays an important role in regulating the availability and mobility of trace metals in aquatic systems (Stumm, 1992). The fact that microbial Fe(III) oxide reduction is known to induce carbonate mineral precipitation suggests that incorporation of metals into carbonates formed during Fe(III) oxide reduction could influence the mobility of trace metal contaminants in anaerobic sedimentary environments through reactions such as

$$(1 - x)\mathrm{Fe}^{2} + x\mathrm{Me}^{2+} + \mathrm{HCO}_3^- = \mathrm{Fe}_{(1-x)}\mathrm{Me}_x\mathrm{CO}_3(\mathrm{s}) + \mathrm{H}^+ \quad (2)$$

$$(1 - x)\mathrm{Ca}^{2+} + x\mathrm{Me}^{2+} + \mathrm{HCO}_3^- = \mathrm{Ca}_{(1-x)}\mathrm{Me}_x\mathrm{CO}_3(\mathrm{s}) + \mathrm{H}^+, \quad (3)$$

where x represents the mole fraction of the trace metal Me^{2+} incorporated into $FeCO_3$(s) or $CaCO_3$(s). The magnitude of metal sequestration via coprecipitation reactions could in principle exceed the capacity of sediment Fe(III) oxides to capture and retain metal contaminants via sorption/surface complexation before the onset of Fe(III) oxide reduction.

The behavior of the fission byproduct ^{90}Sr in groundwater systems is a significant environmental concern at former nuclear weapons manufacturing sites in the United States and abroad (Olsen et al., 1986; Riley et al., 1992; Korobova et al., 1998). At some sites, groundwater ^{90}Sr concentrations exceed the National Interim Drinking Water Regulations limit (8 pCi L^{-1}) by one or more orders of magnitude (Riley et al., 1992). Although substantial chemical retardation of ^{90}Sr relative to mean groundwater velocity is known to occur in contaminated aquifers (Jackson and Inch, 1983), Sr does not sorb as strongly to iron oxide phases as other metal cations (Dzombak and Morel, 1990), and therefore ^{90}Sr is significantly more mobile in the subsurface than other metal-radionuclide contaminants (Sahai et al., 2000).

Abundant evidence exists for the incorporation of Sr into carbonate minerals such as calcite and aragonite, in which Sr can be substituted for Ca in the mineral lattice (Morse and Mackenzie, 1990; Mucci and Morse, 1990). The propensity for Sr to become incorporated into carbonate phases suggests the possibility that microbial Fe(III) oxide reduction could lead to immobilization of Sr in anaerobic subsurface environments through formation of carbonate minerals such as siderite and calcite. To our knowledge, however, the potential for coprecipitation of Sr with siderite, formed biogenically or otherwise, has not yet been evaluated. We report here on an experimental examination of this phenomenon, conducted with a groundwater dissimilatory Fe(III)-reducing bacterium (*Shewanella putrefaciens* strain CN32) in bicarbonate-buffered medium containing synthetic amorphous HFO as a model reactive Fe(III) oxide phase. These studies extend preliminary work on the behavior of 1 mM Sr in HFO reduction systems (Parmar et al., 2001), through experiments with lower levels of Sr (100 and 10 μM) more detailed analysis of the aqueous/solid-phase partitioning of Sr and Fe(II) during HFO reduction. The results demonstrate the potential for substantial Sr incorporation into biogenic siderite (and possibly other biogenic Fe(II) solids), and suggest that carbonate mineral formation coupled to microbial Fe(III) oxide reduction could influence the migration of Sr and other divalent metal contaminants in anaerobic, carbonate-rich sedimentary environments.

2. MATERIALS AND METHODS

2.1. Media and Cultivation

HFO reduction experiments were conducted in bicarbonate-buffered (30 mM $NaHCO_3$) medium containing 4.4 mM NH_4Cl and 0.5 mM KH_2PO_4. The phosphate concentration used was the lowest level required to minimize phase transformations of synthetic HFO (e.g., to goethite; Zachara et al., 2002) during bacterial reduction. The medium was supplemented with nitrilotriacetic acid–complexed trace elements (final concentrations in μM: $AlK(SO_4)_2 \cdot 12H_2O$, 0.21; $CaCl_2 \cdot 2H_2O$, 6.8; $CoCl_2 \cdot 6H_2O$, 4.2; $CuSO_4$, 0.63; H_3BO_3, 1.6; $FeSO_4$, 5.0; $MgSO_4 \cdot 7H_2O$, 122; MnSO4·H_2O, 30; NaCl, 170; $Na_2MoO_4 \cdot 2H_2O$, 1.0; $NaWO_4 \cdot 2H_2O$, 0.76; 1.0 μM; $NiCl_2 \cdot 6H_2O$, 1.0; Na_3NTA, 64) and vitamins as described in Lovley and Phillips (1986). Sodium lactate (20 mM) was used as carbon and energy source in all experiments. Fifty-milliliter portions of culture medium were dispensed into 100-mL serum bottles and bubbled for 30 min with O_2-free N_2:CO_2 (80%:20%), which produced an initial pH of 6.8 and a dissolved IC (DIC) concentration of ~20 mM. Quartz sand (−50 to +70 mesh; Sigma Chemicals) was added to culture medium at a concentration of 100 g L^{-1} before bubbling; preliminary experiments showed that inclusion of the sand prevented formation of mineral precipitates on the bottom of the culture bottles. The bottles were capped with thick butyl rubber stoppers, crimp sealed, and autoclaved at 121°C for 20 min.

A sterile stock suspension of hydrous ferric oxide (HFO) was prepared by neutralizing 0.4 M $FeCl_3 \cdot 6H_2O$ with 1 N NaOH and repeatedly washing the oxide precipitate with sterile distilled water to reduce the Cl^- content (measured by ion chromatography) to <1 mM (Lovley and Phillips, 1986). All solutions and containers were sterilized by autoclaving before HFO preparation. The resulting HFO suspension was purged with sterile, O_2-free N_2 and stored at 4°C. An aliquot of the suspension was added to culture medium to obtain a Fe(III) concentration of 30 to 40 mmol L^{-1}.

$SrCl_2 \cdot 2H_2O$ was added to HFO-containing culture medium from sterile, 100× anaerobic stock solutions to achieve concentrations of ~1.0 mM, 100 μM, or 10 μM. In some experiments, $CaCl_2 \cdot 2H_2O$ was added from a sterile anaerobic stock to a concentration of ~10 mM. A 1- to 2-h equilibration period preceded inoculation of cultures.

S. putrefaciens strain CN32 (Subsurface Microbial Culture Collection; Fredrickson et al., 1998) was grown for 16 h in tryptic soy broth at 37°C on a rotary shaker (150 rpm). Cells were harvested by centrifugation and washed twice in 10 mM 1,4-piperazinediethanesulfonic acid (pH 7.0) in an anaerobic chamber. Direct and viable counts indicated a density of $\sim 5 \times 10^9$ cells mL^{-1} for a typical washed suspension. The cell suspension was added to culture medium at a 1:50 (v/v) ratio, yielding a cell density of $\sim 10^8$ cells mL^{-1}. Duplicate cultures were used in each experiment. All cell additions, transfers, and culture component additions were made via sterile plastic syringes and needles sparged with O_2-free N_2. Culture vessels were incubated statically at 30°C in the dark. Controls consisted of medium that received sterile anaerobic buffer instead of the cell suspension.

2.2. General Analytical Techniques

The concentration of CO_2 in the headspace of culture bottles was determined with a Shimadzu GC-14A gas chromatograph (GC) equipped with a methanizer. After headspace analysis, culture bottles were placed in a Coy anaerobic chamber (98:2 N_2:H_2 atmosphere). A 0.25-mL aliquot was added to a preweighed vial containing 5 mL of 1.0 N HCl for Fe(II) and total Fe analysis as described previously (Roden and Lovley, 1993b). A 1-mL aliquot was removed for pH determination with an Orion model 710A pH meter equipped with a Corning minielectrode. A 1-mL aliquot was added to a sealed, preweighed 6 mL

Wheaton serum vial containing 1 mL of 4% Ultrex nitric acid. Another 1-mL sample was centrifuged inside the chamber for 10 min to pellet particulates. The supernatant was collected and passed through a 0.45-μm filter on the way into a second preweighed, nitric acid–containing 6-mL Wheaton serum vial. These samples (whole and filtered) were allowed to stand overnight. By acidifying the samples, it was assumed that all solid-phase and/or DIC was driven out of solution as CO_2 and into the vial headspace. The CO_2 concentration in a 100-μL sample of the vial headspace was analyzed by GC. The difference between the amount of IC liberated from whole-culture samples (containing particulates) vs. that from filtered samples was assumed to represent the total solid-phase inorganic carbonate content of the cultures, which is designated as IC(s). The ability of this procedure to quantitatively recovery the IC content of carbonate minerals was verified by analyzing a 10 mmol L^{-1} suspension of reagent-grade calcium carbonate. The acidified whole and filtered samples were analyzed for Fe, Sr, and Ca by inductively coupled plasma (ICP) analysis (Leeman Labs).

2.3. Quantification of Metals Associated with Solid-Phase Carbonates

A modification of the citrate–dithionite (CD) extraction of Mehra and Jackson (1958) was used to determine the proportion of the Fe(II), Sr, and Ca associated with carbonate mineral phases vs. other Fe-bearing solids. The alkaline CD extractant (see below) dissolved unreduced HFO and thereby released any sorbed Sr (and Ca) while preserving the stability of the carbonate minerals, leaving them as residual particles that were recovered by filtration. As described in section 3.6, substantial amounts of noncarbonate Fe(II)(s) also remained stable during the alkaline CD extraction, so that this procedure did not provide specific information on the quantity of Fe(II)(s) associated with carbonate minerals. In addition, some portion of the solid-phase Sr and Ca recovered by filtration of the alkaline CD extracts may have been associated with noncarbonate Fe(II)-bearing phases (see section 4.2).

Inside the anaerobic chamber, 1 mL of culture sample was added to a scintillation vial containing 5 mL of anaerobic *N*-2-hydroxyethylpiperazine-*N*'-2-ethanesulfonic acid (HEPES) buffer (0.1 M, pH 8.0) containing 0.3 M Na-citrate. Sodium dithionite (0.025 g) was added to each vial and the contents mixed by swirling. After a 30-min extraction, the samples were passed through a 0.2-μm filter enclosed in a plastic filter holder (Gelman Sciences). The filters, which retained the carbonate mineral precipitates, were washed with 5 mL of the HEPES–citrate buffer. The filters (two per culture bottle) were removed from the holder and processed in one of two ways. One filter was mounted on an aluminum stob by means of a carbon disk for analysis by scanning electron microscopy (SEM). The other filter was placed in a 6-mL Wheaton vial, sealed, and acidified with 2 mL of 4% Ultrex nitric acid. The IC content of the CD-extracted (carbonate) material retained on the filters was determined by GC analysis of the vial headspace; the Sr, Fe, and Ca content was determined by ICP analysis of the nitric acid extract.

The solid-phase speciation of Sr in Ca-free (6.8 μM $CaCl_2 \cdot 2H_2O$ from the trace element solution) cultures without added *S. putrefaciens* cells was examined by the alkaline CD extraction to define the initial disposition of Sr in our culture systems. $SrCl_2 \cdot 2H_2O$ was added at 1.0, 0.1, or 0.01 mM to bottles containing 100 mL of culture medium with quartz sand (100 g L^{-1}), with or without 30 mmol HFO L^{-1}. The cultures were analyzed as described above after 1, 2, and 7 d for total and aqueous Sr, as well as carbonate- and noncarbonate-associated solid-phase Sr.

2.4. X-ray Diffraction

Samples (0.25 mL) collected at the end of the 1 mM Sr experiments were placed on petrographic slides for X-ray diffraction (XRD) analysis. After drying anaerobically overnight, the samples were sealed with ethyl cellulose dissolved in amyl-acetate (8% w:v) to prevent oxidation. Slides were stored under anaerobic conditions until the time of analysis. Analysis was performed with a Phillips APD 3600 automated X-ray powder defractomer (45 kV/40 mA) that used Cu K_α radiation. All samples were analyzed between 2° and 70° (2θ). Diffraction patterns were analyzed by the Jade software package (version 3.0).

2.5. SEM–Energy Dispersive X-ray Spectroscopy

Samples (1 mL) collected at the end of the 100 μM Sr HFO reduction experiments were centrifuged under anaerobic conditions. The supernatant was removed and the pellet resuspended in an equal volume of deionized water. A portion of the washed sample (0.25 mL) was dried on an aluminum stob in the anaerobic chamber. The stobs were stored in the chamber until coated with Au-Pd under vacuum with a Technics Hummer V sputtering coater. A Hitachi S-2500 SEM was used to observe crystal morphology. X-ray energy dispersive spectroscopy (EDS) analyses were conducted with a Noran Instruments EDS unit linked to the SEM.

2.6. Abiotic Coprecipitation Experiments

Two experiments were conducted to examine the potential for incorporation of Sr into chemically precipitated $FeCO_3$(s). Both experiments were conducted at room temperature (22 ± 1°C) in $NaHCO_3$-buffered medium that was identical to that used for the HFO reduction experiments (including quartz sand at 100 g L^{-1}), with the exception that the electron donor, inorganic nutrients, vitamins, and trace elements were omitted. Sr was added from an anaerobic stock solution to achieve a final concentration of 10 μM. In the first experiment, $FeCl_2 \cdot 2H_2O$ was added (from anaerobic stock solutions) to bottles of medium to achieve final concentrations of 1, 2, 5, or 10 mM Fe(II). NaOH was added (from anaerobic stock solutions) at a 1.5:1 or 2:1 mol/L ratio with the $FeCl_2$ to maintain pH values low enough to avoid supersaturation with respect to strontianite. Final pH values ranged from 7.2 to 7.5. Samples were analyzed for total and aqueous IC, Fe(II), and Sr as described above after 1, 10, or 22 d of incubation. In the second experiment, 10 mM $FeCl_2$ + 15 mM NaOH was added to medium containing 10 μM Sr with or without 1 mM $CaCl_2 \cdot 2H_2O$; samples were collected for total and dissolved IC, Fe(II), and Sr analysis after 1, 2, 3, 4, or 6 d of incubation.

2.7. MINEQL+ Calculations

MINEQL+ (version 4.0; Schecher and McAvoy, 1998) was used to compute saturation index (SI) values for metal-carbonate minerals by means of total aqueous metal, DIC, and pH values measured during the HFO reduction experiments. Both major medium components and trace elements (excluding $AlK(SO_4)_2 \cdot 12H_2O$, $CuSO_4$, H_3BO_3, $Na_2MoO_4 \cdot 2H_2O$, and $NaWO_4 \cdot 2H_2O$) were considered in the speciation calculations. Stability constants (log K values) for aqueous complexes were obtained from the MINEQL+ database, with the exception of those for the Fe^{2+}-CO_3^{2-}-H_2O, Sr^{2+}-CO_3^{2-}-H_2O, and Fe^{2+}-NTA^{3-} systems, which were obtained from Bruno et al. (1992), Nordstrom et al. (1990), and Smith and Martell (1997), respectively. Stability constants for lactate-metal ion complexes were obtained from Smith and Martell (1997). A log K of 2.0 was used for lactate-Fe(II) complexes, equal to the average value for several divalent cations (Smith and Martell, 1997). The solubility products for carbonate minerals were those included in the MINEQL+ database. Activity corrections based on computed ionic strengths were included in all SI calculations.

3. RESULTS

3.1. Influence of Sr on Bacterial HFO Reduction

An experiment was conducted to determine whether Sr had any detrimental effect on HFO reduction by *S. putrefaciens* CN32. The presence of 1 mM Sr led to a detectable but minor (~10%) decrease in HFO reduction over a 30-d incubation period (data not shown). Similar experiments performed with another *Shewanella* species (*S. alga* strain BrY) also demonstrated only a minor negative influence of 1 mM Sr on HFO reduction (Parmar et al., 2000; M. Leonardo, unpublished data).

Table 1. Sr recovered in the solid-phase at the beginning and end of low-Ca and Ca-amended HFO reduction experiments. Each value is the mean (range) of duplicate cultures.

System	Experiment	% Sr in solid phase[a] Beginning	End
Ca free	1 mM Sr	55.3 (1.0)	88.6 (0.7)
	100 μM Sr	80.9 (2.2)	99.5 (0.1)
	10 μM Sr	87.1 (8.4)	96.4 (1.5)
10 mM Ca	1 mM Sr	23.2 (2.5)	24.7 (0.7)
	100 μM Sr	28.1 (1.4)	27.4 (1.7)
	10 μM Sr	32.6 (5.1)	33.6 (0.5)

[a] Computed from the difference between the Sr content of whole (unfiltered) and 0.2-μm-filtered culture samples.

3.2. Initial Disposition of Sr

Approximately 45% of total Sr was in solution at the start of HFO reduction experiments in Ca-free 1 mM Sr cultures, whereas less than 20% of total Sr was initially in solution in Ca-free 100 μM and 10 μM Sr systems (Table 1). A substantially greater amount of total Sr was initially in solution in Ca-amended cultures (Table 1). Analysis of uninoculated cultures by alkaline CD extraction (see "Materials and Methods") showed that virtually none of the initial solid-phase Sr (Sr(s)) was associated with carbonates 2 to 7 d after Sr addition (Table A1). These findings indicate that the Sr(s) present at the start of the experiments was sorbed to HFO and bacterial cell surfaces. It can be inferred from studies of Sr sorption to HFO and *S. putrefaciens* CN32 cell surfaces (Small et al., 1999) that at the cell densities used in our experiments, Sr sorption by bacterial surfaces was minor compared with sorption by HFO.

3.3. Behavior of Sr during HFO Reduction

Preliminary experiments with uninoculated 1 mM Sr cultures failed to show systematic changes in aqueous Sr (or Ca in 10 mM $CaCl_2$-amended systems) concentration over a 1-month period (Table A2). Thus, changes in aqueous/solid-phase Sr and Ca partitioning in cultures inoculated with *S. putrefaciens* can be attributed to bacterial HFO reduction activity. A consistent pattern of Sr partitioning between the aqueous and solid phase was observed during active HFO reduction in Ca-free cultures with different levels of total Sr. Sr was released to solution in parallel with Fe(II)(aq) during the early stages of HFO reduction (Figs. 1A,B). Between 75% (10 μM Sr system) and 93% (1 mM Sr system) of the initially sorbed Sr was released. Subsequent to the initial period of mobilization, Sr and Fe(II)(aq) were removed from solution in parallel with accumulation of IC(s), a steady rise in culture pH (Fig. 1C), and a change in the color of the suspension from brownish-black to whitish-gray associated with the production of siderite (see below). Aqueous Sr concentrations in the 100 μM and 10 μM Sr cultures were close to the detection limit of 0.5 μM at the end of the incubations. The amount of Sr immobilized (i.e., not present in solution) at the end of the Ca-free experiments (89 to 99%; Table 1) was greater than the amount of Sr, which was sorbed to HFO and bacterial cell surfaces at the start of the experiments (55 to 87%).

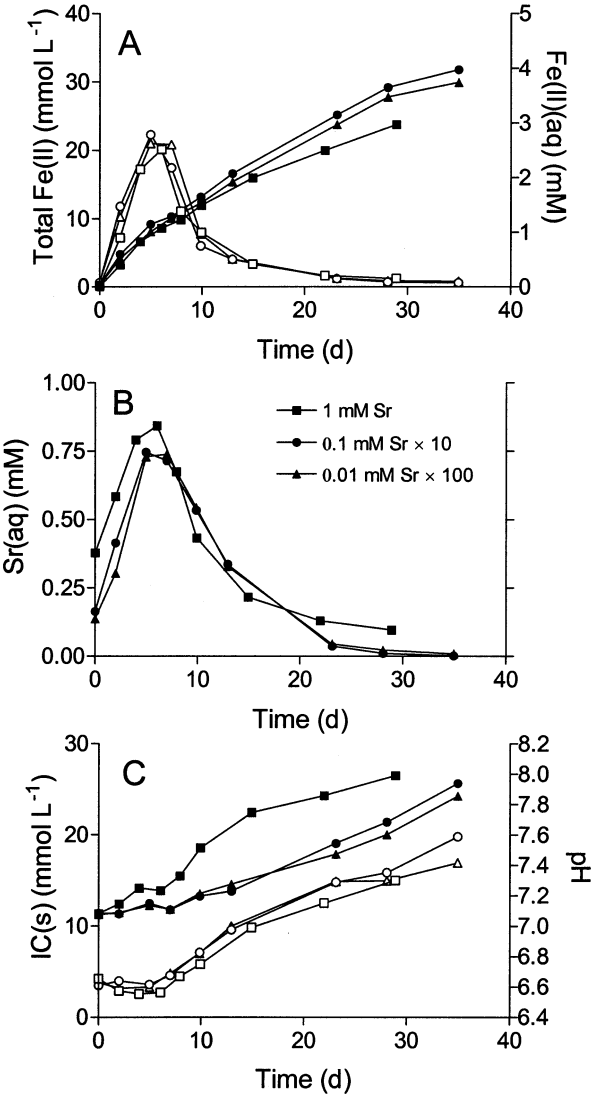

Fig. 1. Changes in aqueous and solid-phase chemical conditions during HFO reduction in Ca-free cultures containing 1 mM (squares), 100 μM (circles), or 10 μM (triangles) Sr. (A) Total (solid symbols) and aqueous (open symbols) Fe(II). (B) Aqueous Sr. (C) pH (solid symbols) and IC(s) (open symbols). Symbols represent means of duplicate cultures; the range of duplicates was $<$10% of the mean.

As in the Ca-free cultures, Sr and Fe(II) were released to solution during the initial stages of HFO reduction in Ca-amended cultures (Figs. 2A,B). However, the degree of subsequent Sr immobilization was dramatically reduced compared with Ca-free cultures. After $\sim$5 d of incubation, aqueous Ca concentrations began to decline in parallel with Fe(II)(aq), indicating the onset of $FeCO_3$(s) and $CaCO_3$(s) precipitation. The onset of carbonate precipitation was evidenced by the accumulation of whitish precipitates and accompanied by a sharp increase in IC(s) and a noticeable drop in culture pH (Fig. 2C). pH values increased only slightly after initiation of carbonate precipitation. The fraction of Sr not present in solution at the end of the Ca-amended experiments was similar to the amount of Sr, sorbed to HFO and bacterial cell surfaces at the start of the experiments (Table 1).

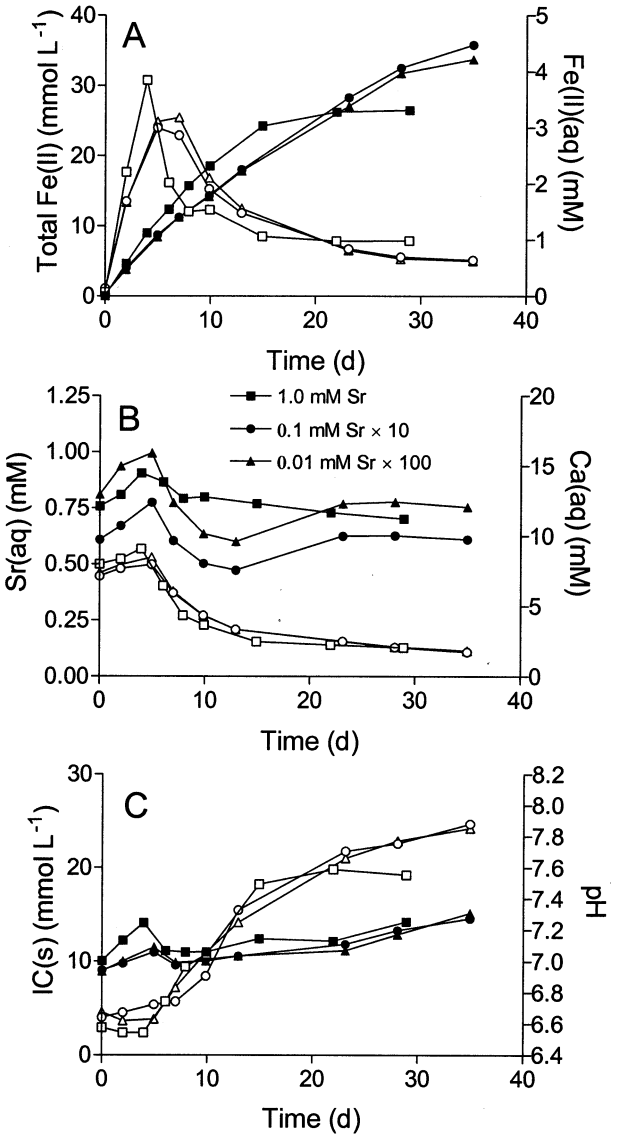

Fig. 2. Changes in aqueous and solid-phase chemical conditions during HFO reduction in Ca-amended (10 mM) cultures containing 1 mM (squares), 100 μM (circles), or 10 μM (triangles) Sr. (A) Total (solid symbols) and aqueous (open symbols) Fe(II). (B) Aqueous Sr (solid symbols) and Ca (open symbols). (C) pH (solid symbols) and IC(s) (open symbols). Symbols represent means of duplicate cultures; the range of duplicates was $<$ 10% of the mean.

3.4. SI Calculations

MINEQL+ calculations indicated that the aqueous phase of the 1 mM Sr cultures was oversaturated with respect to strontianite throughout the experiments (SI = 0.2 to 1.4) (Figs. 3A,B). In contrast, the 100 μM and 10 μM Sr culture systems were at all times undersaturated with respect to strontianite. The Ca-free systems became increasingly undersaturated with respect to strontianite as Sr was removed from solution during HFO reduction, whereas SI values remained relatively constant in the Ca-amended cultures in which much less Sr immobilization took place. All culture systems were substantially oversaturated with respect to siderite throughout the experiments (Fig. 3C). The initial increase and subsequent decline in SI values for siderite paralleled the time course of Fe(II)(aq) concentration during HFO reduction (Figs. 1A, 2A). The Ca-amended systems were continuously oversaturated with respect to calcite, although conditions approached equilibrium as $CaCO_3$(s) precipitated during the course of the experiments (Fig. 3D).

3.5. XRD and SEM-EDS Analyses

Siderite was identified by XRD as the major end product of HFO reduction in Ca-free 1 mM Sr cultures (Fig. 4C) ; no other crystalline Fe(II)-bearing minerals (e.g., magnetite, vivianite) were detected. XRD analysis suggested that ankerite, a Fe(II)-substituted analog of dolomite (Lippman, 1973), was the primary mineral formed in Ca-amended HFO reduction cultures (Fig. 5C). EDS analysis during SEM revealed the presence of Sr associated with carbonate phases in both Ca-free and Ca-amended cultures (Figs. 4B, 5B).

3.6. Wet-Chemical Speciation of Solid-Phase Sr, Ca, and Fe(II)

Samples collected at the end of the HFO reduction experiments were extracted with alkaline CD reagent and filtered to separate Sr, Ca, and Fe(II) putatively associated with carbonates from other solid phases (see Materials and Methods). Values for IC(s) content determined by this procedure agreed well (94.6 $\pm$ 5.8%, n = 12) with the difference between the amount of IC released by acidification of whole versus filtered culture samples (Table 2), which verified the ability of the CD extraction to quantitatively recover solid-phase carbonate minerals produced during HFO reduction.

The quantity of Sr recovered in particulate form after CD extraction was equal to 46 and 59% of the total solid-phase Sr (as determined by analysis of whole vs. 0.2 μM-filtered culture samples) content of Ca-free and Ca-amended 1 mM Sr cultures, respectively (Table 2). A larger fraction (88 to 100%) of Sr(s) was retained by filtration after CD extraction of materials from 100 μM and 10 μM Sr cultures (Table 2). The relative recovery of particulate Ca after CD extraction paralleled that of particulate Sr in Ca-amended cultures: recovery was substantially less in 1 mM Sr systems (56% of total Ca(s)) compared with 100 μM (85% of total Ca(s)) and 10 μM (79% of total Ca(s)) (Table 2).

The difference between the total Fe(II)(s) and IC(s) contents of Ca-free cultures (Table 2) suggested that appreciable amounts of noncarbonate Fe(II)(s) were produced during HFO reduction, which amounted to 11.2 $\pm$ 2.1 mmol L^{-1} (mean $\pm$ SD, n = 6) of noncarbonate Fe(II)(s), equivalent to 38.6 $\pm$ 3.8% of total Fe(II)(s). For these calculations, the carbonate-associated Sr(s) content of the particulate materials, as determined by the CD extraction procedure, was subtracted from total IC(s) values to estimate the quantity of IC(s) directly associated with $FeCO_3$(s). Analogous calculations for Ca-amended cultures, which included a correction for the estimated contribution of $CaCO_3$(s) to IC(s), indicated the formation of 13.6 $\pm$ 2.7 mmol L^{-1} of noncarbonate Fe(II)(s), equivalent to 43.1 $\pm$ 3.0% of total Fe(II)(s).

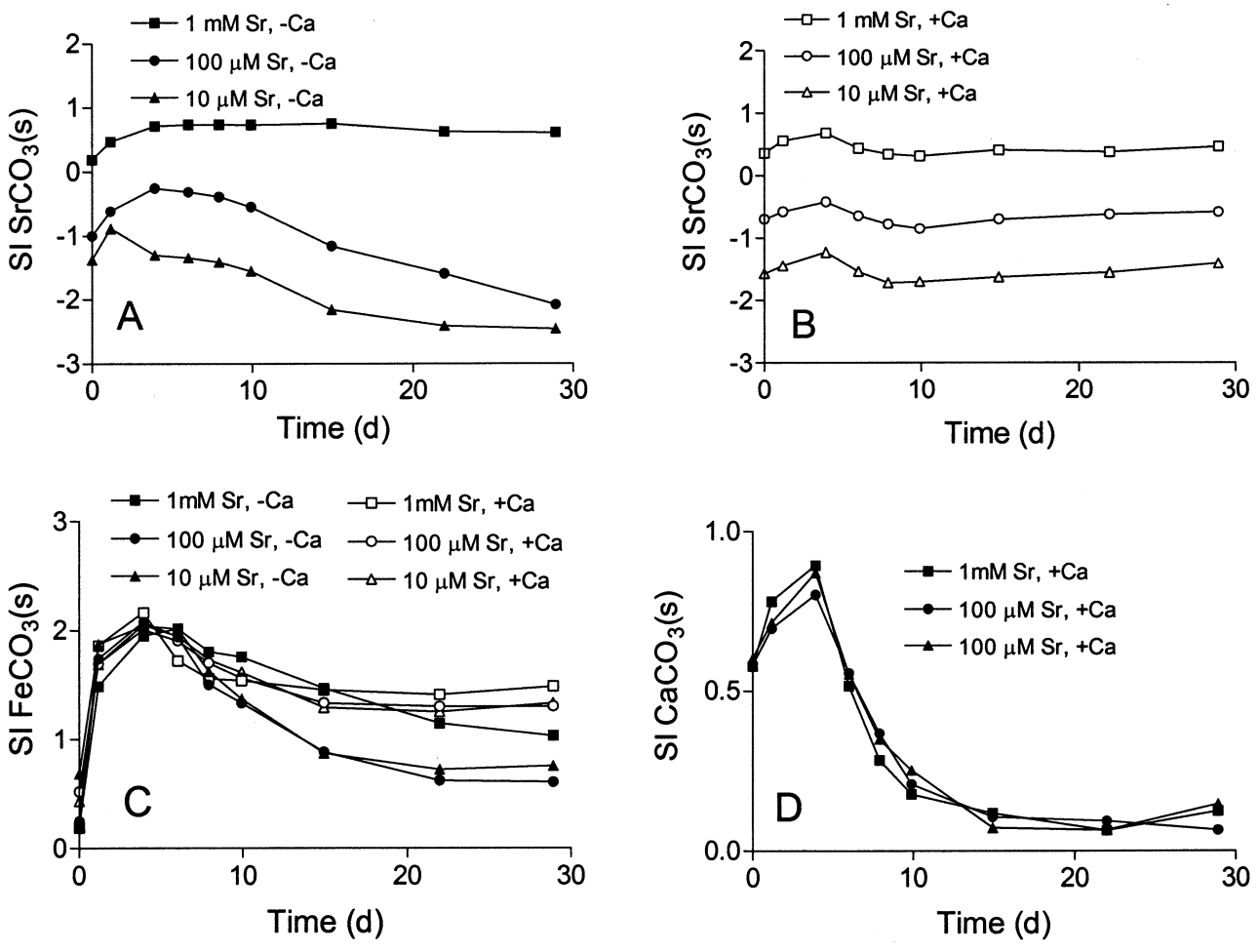

Fig. 3. SI calculations (MINEQL+) for $SrCO_3$(s) (strontianite) (A, B), $FeCO_3$(s) (siderite) (B), and $CaCO_3$(s) (calcite) (D) in Ca-free (−Ca; solid symbols) and Ca-amended (+Ca, open symbols) HFO reduction experiments containing 1 mM (squares), 100 μM (circles), or 10 μM Sr (triangles). Calculations were performed using average metal cation, DIC, and pH values for duplicate cultures. SI calculations for $CaCO_3$(s) were conducted only for cultures containing 10 mM Ca.

Fe(II)(s) recovered by filtration after alkaline CD extraction accounted for ~90% of the total Fe(II)(s) (whole minus filtered), with no major differences observed among cultures containing different levels of Sr and Ca (Table 2). Because noncarbonate Fe(II)(s) accounted for a significant fraction of total Fe(II)(s), these results indicate that most of the noncarbonate Fe(II)(s) remained stable during the CD extraction. Assuming that carbonate-associated Fe(II)(s) (i.e., siderite and ankerite) remained completely undissolved during CD extraction, the quantity of Fe(II)(s) lost during CD extraction (~2.5 and 3.5 mmol Fe(II)(s) L^{-1} in the Ca-free and Ca-amended cultures, respectively) averaged ~25% (24.7 ± 17.0, n = 12) of noncarbonate Fe(II)(s).

3.7. Abiotic Coprecipitation Experiments

Abiotic Sr-Fe(II) coprecipitation experiments were conducted in reaction systems having aqueous phase conditions (pH, DIC, Fe(II), Sr) comparable to those present in the HFO reduction experiments (see "Materials and Methods"). Formation of a whitish precipitate was observed when $FeCl_2$ (1 to 10 mM) was added to anoxic $NaHCO_3$ solutions, and this mineral precipitation was associated with a rapid decline in Fe(II)(aq) concentration (Fig. 7A). XRD and SEM-EDS analysis confirmed the formation of siderite (data not shown). Sr was removed from solution in parallel with Fe(II) during siderite precipitation (Fig. 7B). In a second experiment, the presence of 1 mM Ca suppressed coprecipitation of Sr with ~10 mmol L^{-1} siderite (Fig. 8A), whereas Ca was removed from solution in a manner comparable to that observed for Sr in the absence of Ca (Fig. 8B).

4. DISCUSSION

4.1. End Products of Bacterial HFO Reduction

Wet-chemical determinations (Figs. 1, 2) together with XRD and SEM analyses (Figs. 4, 5) showed that siderite and ankerite were major end products of HFO reduction in Ca-free and Ca-amended cultures, respectively. The siderite rhombs formed in Ca-free cultures (Fig. 4A) were morphologically similar to those described by Mortimer and Coleman (1997) and

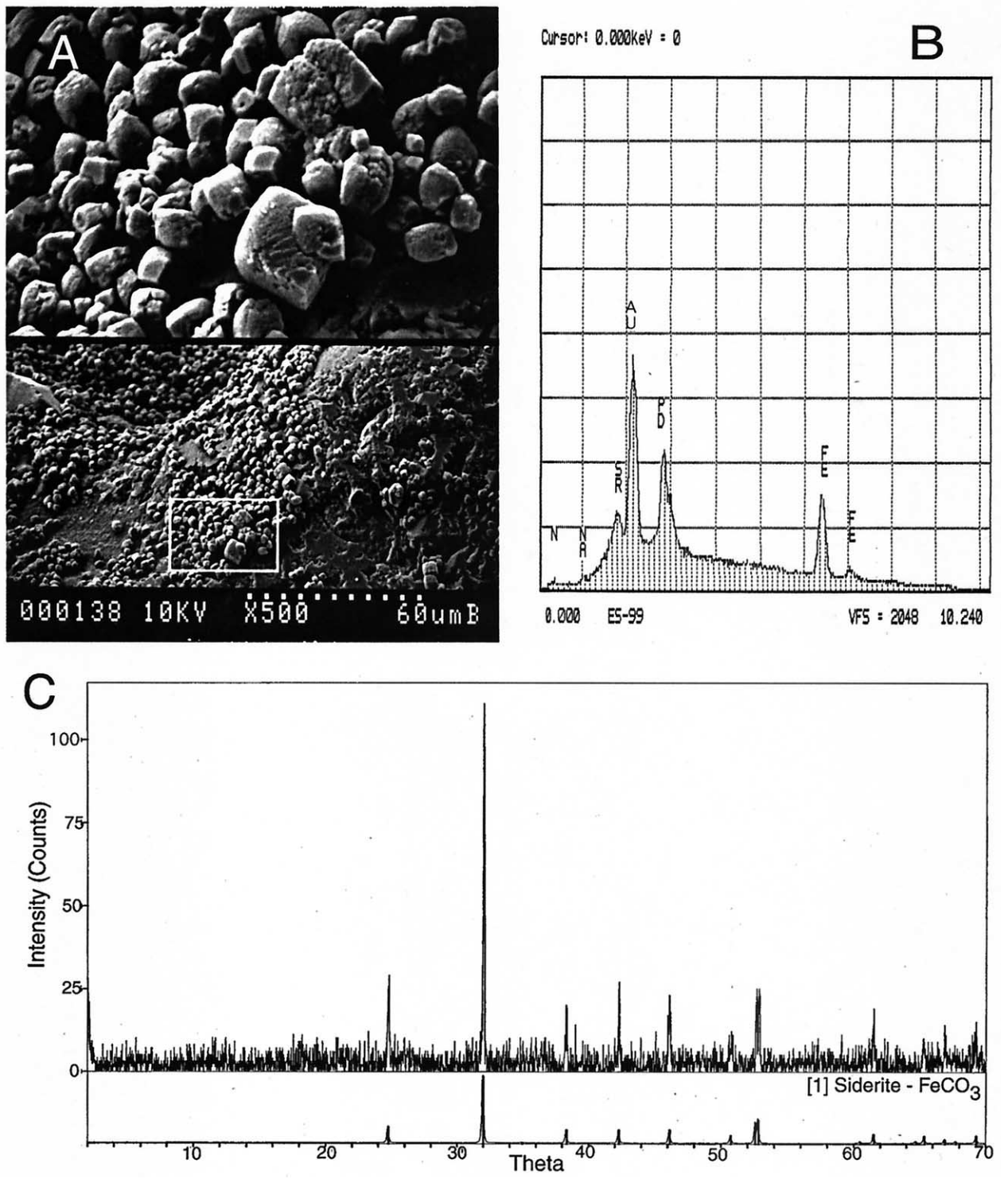

Fig. 4. Carbonate minerals formed during HFO reduction in Ca-free culture systems. (A) SEM micrograph showing CD-treated minerals (bar = 60 μm, lower panel; 6 μm, upper panel). (B) EDS spectrum of the minerals shown (A). The Au and Pd peaks are artifacts of the Au-Pd coating of the sample before SEM analysis. (C) XRD spectrum of untreated minerals. The top spectrum represents the analyzed sample; the lower spectrum shows peaks characteristic of pure siderite.

Fredrickson et al. (1998) for bicarbonate-buffered HFO reduction systems similar to those employed in this study.

Ankerites are known to occur with some frequency as rock-forming minerals, and chemical analysis of siderites from sedimentary formations generally show considerable amounts of Ca and Mg (Lippman, 1973; Pye, 1984; Mozley and Carothers,

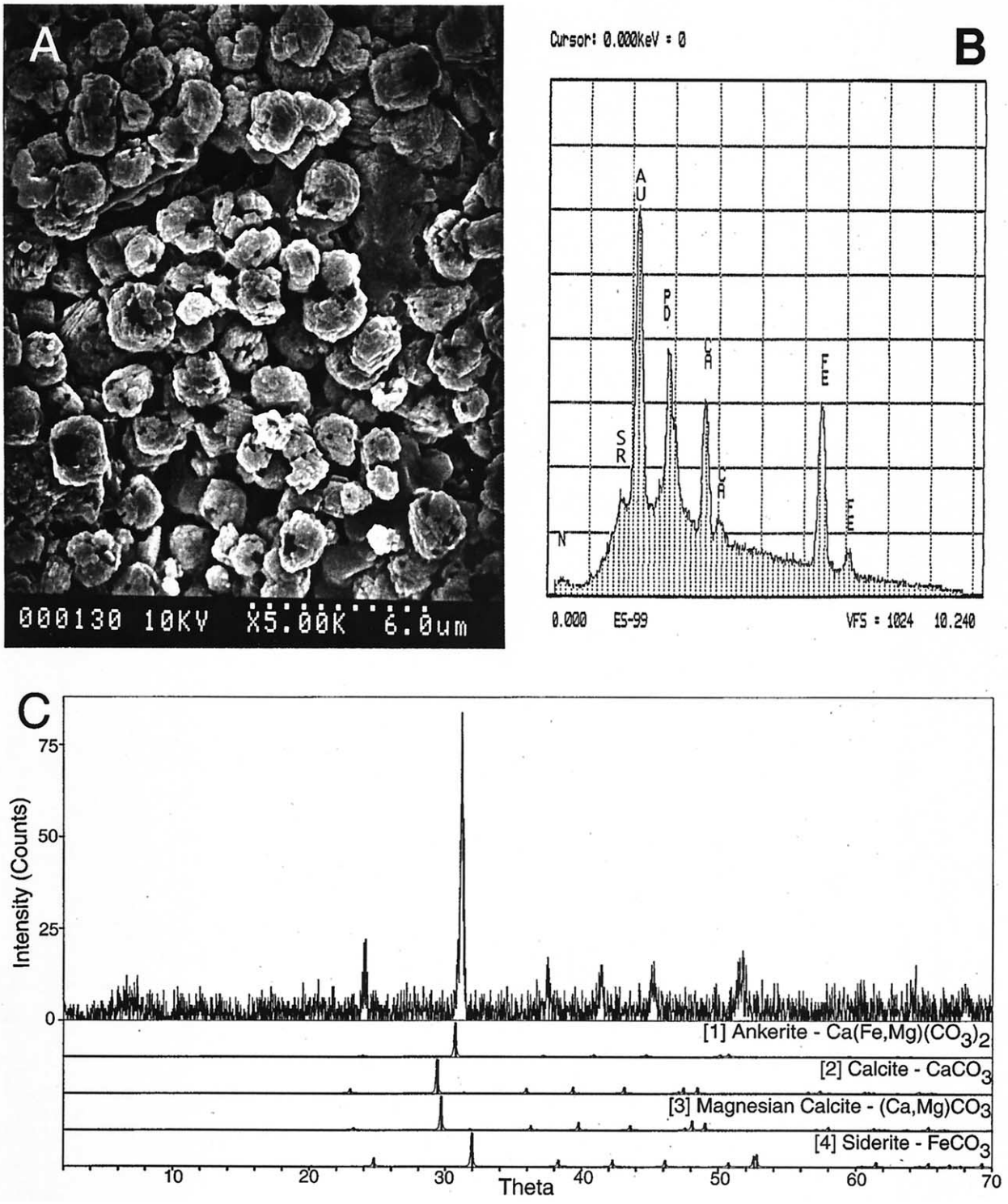

Fig. 5. Carbonate minerals formed during HFO reduction in 10 mM Ca systems. (A) SEM micrograph showing CD-treated minerals (bar = 6 μm). (B) EDS spectrum of the minerals shown (A). The Au and Pd peaks are artifacts of the Au-Pd coating of the sample before SEM analysis. (C) XRD spectrum of untreated minerals. The top spectrum represents the analyzed sample; the lower spectra shows peaks characteristic of pure minerals listed.

1992). Incorporation of Ca (as well as Mg and Mn) into siderite formed during bacterial HFO reduction has been previously observed (Mortimer and Coleman, 1997; Mortimer et al., 1997), although we are unaware of previous XRD documentation of ankerite formation during bacterial HFO reduction. The slight peak shift observed in relation to the reference spectrum for ankerite (Fig. 5C) is probably the result of the relatively high concentration of Fe(II) within the mineral (Lippman, 1973).

Table 2. Composition of solid-phase materials recovered by filtration at the end of the Ca-free (−Ca) and Ca-amended (+Ca) HFO reduction experiments. Each value is the mean of duplicate cultures; the range of duplicate cultures was typically <10% of the mean. Units are mmol L^{-1}.

	Fe(II)				IC[c]			Ca			Sr		
Experiment	CD[a]	WvF[b]	CD/WvF	Noncarb Fe(II)(s)[d]	CD	WvF	CD/WvF	CD	WvF	CD/WvF	CD	WvF	CD/WvF
1 mM Sr, −Ca	22.2	23.6	0.938	8.86	15.1	15.1	1.000	NA[e]	NA	NA	0.346	0.748	0.462
100 μM Sr, −Ca	28.6	32.3	0.885	12.3	17.7	20.1	0.884	NA	NA	NA	0.0751	0.0857	0.876
10 μM Sr, −Ca	28.1	30.6	0.909	12.3	17.9	18.3	0.982	NA	NA	NA	0.00974	0.0102	0.951
Mean			0.914	11.2			0.956						
SD (n = 6)			0.071	2.1			0.083						
10 mM Sr, +Ca	20.7	25.5	0.813	10.4	17.8	19.2	0.927	3.93	7.05	0.559	0.139	0.238	0.585
100 μm Sr, +Ca	31.1	35.0	0.892	16.2	23.1	24.7	0.935	5.93	6.96	0.853	0.0256	0.02323	1.100
10 μM Sr, +Ca	31.5	33.4	0.943	14.2	23.3	24.7	0.946	5.40	6.86	0.787	0.00381	0.00404	0.942
Mean			0.883	13.6			0.936						
SD (n = 6)			0.068	2.7			0.017						
Grand mean			0.898	12.4			0.946						
SD (n = 12)			0.068	2.6			0.058						

[a] From analysis of particulate materials retained by filtration from alkaline citrate–dithionite (CD) extraction.
[b] From analysis of whole vs. filtered (WvF) culture samples.
[c] Inorganic carbon.
[d] Noncarbonate solid-phase Fe(II), computed as the difference between total (WvF) solid-phase Fe(II) and total (WvF) solid-phase inorganic carbon, with corrections for the estimated (CD extraction) carbonate-associated Sr and Ca contents of the particulate materials.
[e] Not applicable.

The wet-chemical speciation of solid-phase Fe(II) conducted at the end of the HFO reduction experiments indicated the formation of appreciable quantities (~40% of total Fe(II)(s)) of noncarbonate Fe(II)(s). Because most of the HFO content of the cultures was reduced by the end of the experiments (88.1 ± 0.9% and 93.0 ± 1.1% for Ca-free and Ca-amended cultures, respectively), magnetite (Fe_3O_4; Fe(II):Fe(III) = 0.5:1), if present, could have accounted for ≤ 20% (~2 to 3 mmol Fe(II) L^{-1}) of the noncarbonate Fe(II)(s). The apparent absence of major magnetite formation is supported by first, the lack of XRD detection of this mineral phase (or any others besides siderite and ankerite; Figs. 4 and 5); and second, the fact that no systematic decline in total 0.5 M HCl-extractable Fe was observed during HFO reduction (data not shown), which was shown by Fredrickson et al. (1998) to occur as a result of magnetite production during HFO reduction by *S. putrefaciens* CN32. Because the culture medium contained only 0.5 mM KH_2PO_4, the maximum amount noncarbonate Fe(II)(s) that could have been present in the form of vivianite ($Fe_3(PO_4)_2$(s)) was 0.75 mmol Fe(II) L^{-1}, less than 10% of total noncarbonate Fe(II)(s)). These considerations indicate that the majority of the noncarbonate Fe(II)(s) produced in our experiments cannot be accounted for by magnetite and vivianite, which are known from previous studies (Lovley et al., 1987; Roden and Lovley, 1993a; Fredrickson et al., 1998) to be dominant end products of HFO reduction.

Although the identity of the majority of noncarbonate Fe(II)(s) generated in our experiments remains unclear, we speculate that poorly crystalline (i.e., X-ray amorphous), mixed Fe(II)-Fe(III) hydroxy compounds (green rusts) can account for the majority of such phases. Both field (Trolard et al., 1997; Genin et al., 1998, 2001) and laboratory (Fredrickson et al., 1998; Parmar et al., 2001; Ona-Nguema et al., 2002; Zachara et al., 2002) studies have demonstrated the potential for formation of such compounds under bacterial Fe(III) oxide reducing conditions. Concentrations of Fe(III) remaining in the Ca-free and Ca-amended cultures averaged 3.91 ± 0.58 and 2.48 ± 0.68 mmol L^{-1} (n = 6), respectively. Given these levels of residual Fe(III), Fe(II):Fe(III) ratios of 2.9 and 5.5 in mixed Fe(II)-Fe(III) hydroxy compounds would be required to account for the 11.2 ± 2.1 and 13.6 ± 2.7 mmol L^{-1} of noncarbonate Fe(II)(s) in the Ca-free and Ca-amended cultures, respectively. Although Fe(II):Fe(III) ratios of this magnitude are not typical of green rusts produced by $Fe(OH)_2$ oxidation in carbonate-buffered medium (Hansen, 1989; Genin et al., 2001), the formation of mixed Fe(II)-Fe(III) phases with relatively high Fe(II):Fe(III) ratios was indicated in studies of bacterial HFO (Parmar et al., 2001) and lepidocrocite (Ona-Nguema et al., 2002) reduction in which a large fraction of the total Fe(III) oxide content of the cultures was reduced.

4.2. Mechanisms of Sr Immobilization in Ca-Free HFO Reduction Systems

4.2.1. Strontianite Precipitation

The aqueous phase of the 1 mM Sr systems was saturated with respect to strontianite from the outset of the HFO reduction experiments (Figs. 3A,B), although wet-chemical analysis of uninoculated cultures showed no evidence of strontianite precipitation in the absence of HFO reduction activity. SI values for strontianite increased three- to fourfold (~0.5 SI units) during HFO reduction in Ca-free cultures. Therefore, one possible mechanism for Sr immobilization in these cultures was precipitation of strontianite inducted by alkalinity generation during HFO reduction. Earlier studies also suggested that strontianite precipitation may have contributed to Sr immobilization in 1 mM Sr HFO reduction systems (Parmar et al., 2000). Although strontianite was not detected by XRD analysis of carbonate phases produced in these studies (e.g., Fig. 4C), the relative abundance of Sr compared with Fe (~5 wt%) was

probably not high enough to permit detection even if substantial amounts of $SrCO_3$(s) were produced.

In contrast to the 1 mM Sr systems, the aqueous phase remained undersaturated with respect to strontianite throughout the 100 μM Sr and 10 μM Sr HFO reduction experiments. These results suggest that some mechanism other than direct $SrCO_3$(s) precipitation was responsible for the extensive incorporation of Sr into carbonate minerals in the 100 μM Sr and 10 μM Sr Ca-free culture systems.

4.2.2. Coprecipitation with Siderite

The well-known potential for coprecipitation of trace metals with major carbonate mineral phases, including siderite (Thornber and Nickel, 1976), suggests that coprecipitation of Sr with siderite could explain the parallel behavior of Sr(aq) and Fe(II)(aq) during HFO reduction in the 100 μM Sr and 10 μM Sr Ca-free cultures (Fig. 1A), and the recovery of Sr with carbonate phases (CD extraction) at the end of the experiments (Table 2). The close correlation between Sr(aq) and Fe(II)(aq) in Ca-free 1 mM Sr systems suggests that coprecipitation of Sr with siderite may have also occurred in conjunction with (or in place of) direct $SrCO_3$(s) precipitation in these cultures.

The Sr(aq) and Fe(II)(aq) data in Figure 1A were analyzed according to the integrated form of the Doerner-Hoskins relation (Doerner and Hoskins, 1925) for heterogeneous coprecipitation of trace elements with major (carrier) elements (Morse and Mackenzie, 1990; Mucci and Morse, 1990):

$$D_{D-H} = \ln([Tr]_0/[Tr]_f)/\ln([Cr]_0/[Cr]_f) \quad (4)$$

where [Tr] and [Cr] are the concentrations of the trace (Sr) and carrier (Fe(II)) components in solution before (0) and after (f) crystallization, respectively, and D_{D-H} is the Doerner-Hoskins partition coefficient. Rearrangement of Eqn. 4 permits estimation of D_{D-H} from the slope of a plot of $\ln([Cr]_0/[Cr]_t)$ vs. $\ln([Tr]_0/[Tr]_t)$, where $[Tr]_0$ and $[Cr]_0$ represent aqueous metal concentrations measured at the point in time when carbonate mineral precipitation began (after 5 to 7 d of incubation; Figure 1C), and $[Tr]_t$ and $[Cr]_t$ represent aqueous metal concentrations at various times during carbonate precipitation. Although correlations between the mole fraction of Sr in precipitated solids and the aqueous-phase Sr:Fe(II) ratio were observed in these experiments (data not shown), it was not appropriate to analyze the data according to the classical homogeneous coprecipitation framework (Morse and Bender, 1990), because the aqueous concentrations of both Fe(II) and Sr changed dramatically during mineral precipitation, and because mineral recrystallization is not likely to have occurred at the temperature of our experiments.

The Fe(II)(aq) and Sr(aq) data from Figure 1A ($t > 5$ to 7 d) conformed reasonably well to the Doerner-Hoskins relation (Fig. 6A). However, the loss of Sr(aq) from solution was retarded relative to loss of Fe(II)(aq) during the initial stages of mineral precipitation in the 100 μM and 10 μM Sr systems. To obtain a D_{D-H} value for Sr coprecipitation with siderite during HFO reduction that could be compared with values for other trace metal-siderite coprecipitation systems (see below), pooled data from the Ca-free experiments were fit to Eqn. 4 for $\ln([Fe(II)aq)_0/[Fe(II)(aq)])$ values greater than 1, where the relationship between $\ln([Sr(aq)_0/[Sr(aq)])$ and $\ln([Fe(II)(aq)_0/[Fe(II)(aq)])$ was generally linear (Fig. 6A). This approach yielded D_{D-H} value of 1.81 $\pm$ 0.15 (r^2 = 0.94).

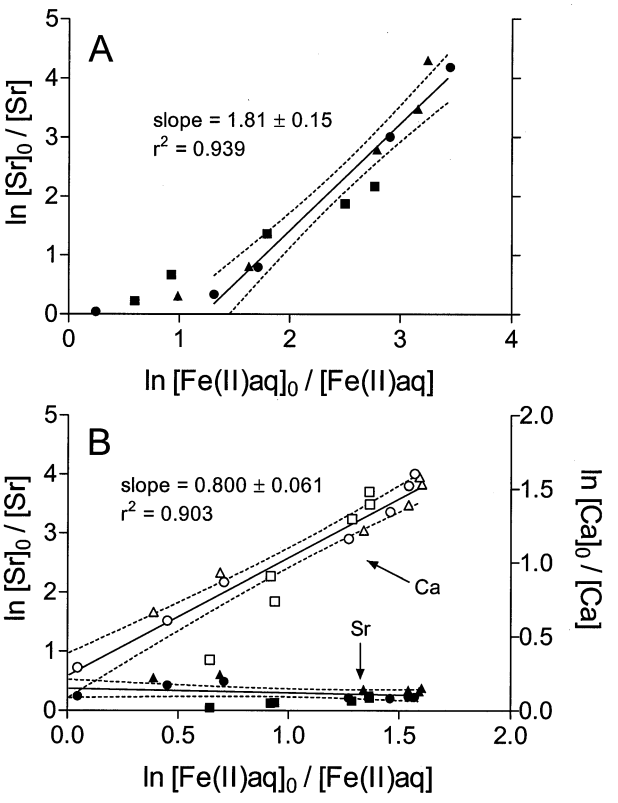

Fig. 6. Doerner-Hoskins analysis of Fe(II)(aq)-Sr(aq) (Ca-free experiments; A) and Fe(II)(aq)-Sr(aq)-Ca(aq) (10 mM Ca experiments; B) from HFO reduction experiments (Figs. 1, 2). The plots include data from after the initiation of major carbonate mineral formation ($t > 5$ to 7 d). Solid and open symbols in (B) show data for Sr and Ca, respectively. Symbols represent means of duplicate cultures; the range of duplicates was <10% of the mean. Solid lines show results of linear least-squares regression analyses; dashed lines indicate the 95% confidence interval for the regression.

Abiotic coprecipitation experiments were conducted to verify the potential for coprecipitation of Sr with siderite. These experiments were carried out in the absence of electron donor, inorganic nutrients, vitamins, and trace elements so as to explicitly demonstrate the potential for coprecipitation of Sr with $FeCO_3$(s). The Fe(II)(aq) and Sr(aq) data conformed generally to the Doerner-Hoskins relation, yielding a mean D_{D-H} value of 0.143 $\pm$ 0.018 (r^2 = 0.57) for pooled data from systems amended with different levels of $FeCl_2$ (Fig. 7B). D_{D-H} values computed (Eqn. 4) by using individual data points from the different $FeCl_2$ systems increased systematically from ~0.05 to 0.4 with increasing rate and quantity of $FeCO_3$(s) precipitation (Fig. 7B, inset).

A study by Rimstidt et al. (1998) developed a framework for calculating theoretical and experimental solid-solution partition coefficients (K_d and K_d' values, respectively) for coprecipitation of trace elements with calcite and siderite, based on the McIntire (1963) model for equilibrium solid solution formation and experimental partition coefficient data from the literature. Predicted K_d' values take into account the effects of surface-site and boundary-layer-related process on trace element partition-

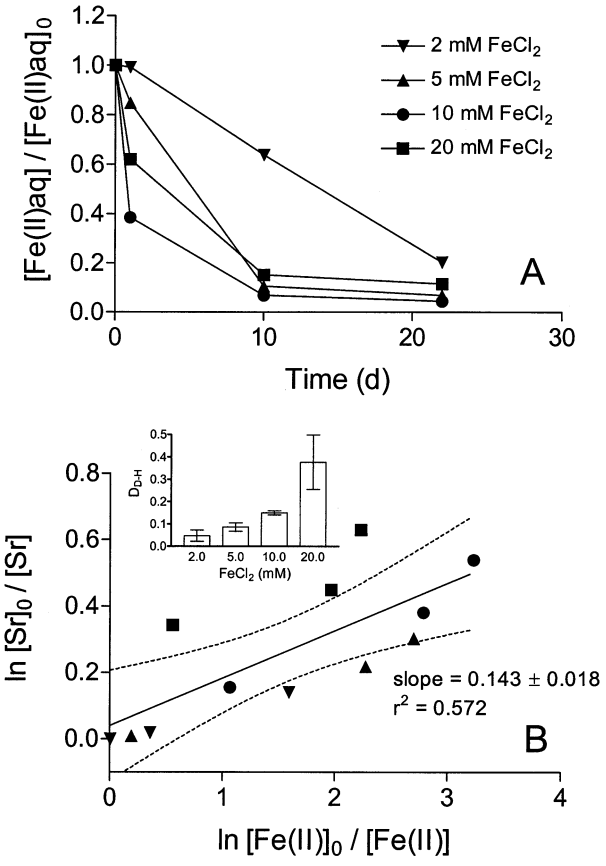

Fig. 7. (A) Time course of Fe(II)(aq) concentration (normalized to initial concentration) from abiotic Fe(Sr)CO_3 coprecipitation experiment (different levels of $FeCl_2$ added to 30 mM $NaHCO_3$, pH 6.8, containing 10 μM $SrCl_2$; see Materials and Methods). Each symbol represents the mean of duplicate samples from a single reaction system. (B) Doerner-Hoskins analysis of Fe(II)(aq)-Sr(aq) data for abiotic coprecipitation experiment. Solid line shows result of linear least-squares regression analysis; dashed lines indicate the 95% confidence interval for the regression. Inset shows mean (±SD) $D_{D\text{-}H}$ (see text) values computed from individual time points (n = 3) for systems amended with different levels of $FeCl_2$.

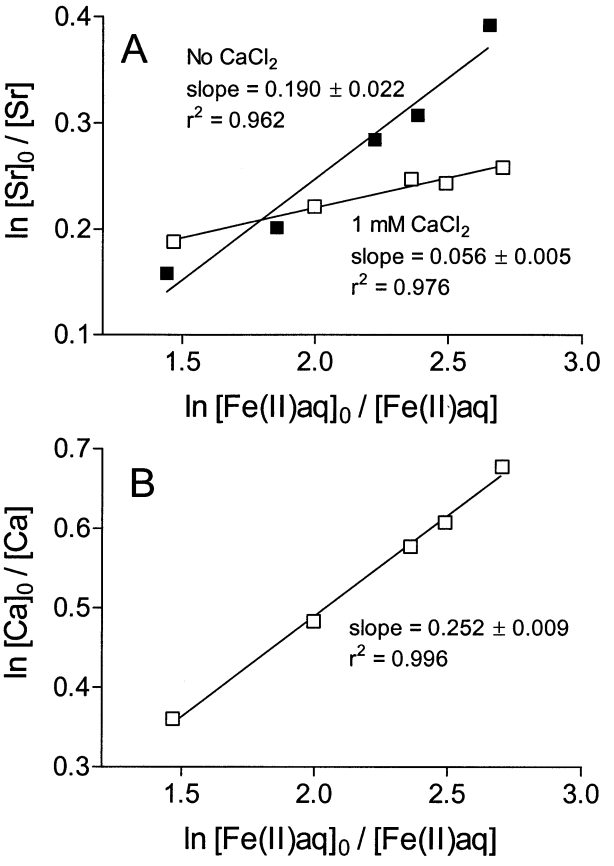

Fig. 8. Analysis of Fe(II)(aq)-Sr(aq)-Ca(aq) data from abiotic Fe(Sr, Ca)CO_3 coprecipitation experiment (10 mM $FeCl_2$ added to 30 mM $NaHCO_3$, pH 6.8, containing 10 μM $SrCl_2$ ± 1 mM $CaCl_2$ and sampled after 1, 2, 3, 4,and 6 d; see Materials and Methods) according to the Doerner-Hoskins relation for heterogeneous coprecipitation. Open symbols = 1 mM $CaCl_2$; solid symbols = no $CaCl_2$. Each symbol represents the mean of duplicate samples from a single reaction system.

ing, whereas predicted K_d values are thermodynamic parameters for equilibrium solid solution formation. Because we are unaware of any previous experimental data on the partitioning of Sr into siderite, the following relationships developed in Rimstidt (1998) were used to estimate K_d' and K_d values for Sr partitioning into siderite to permit comparison with our experimental results:

$$K_d' = 4.1\left(\frac{K_{FeCO_3}}{K_{SrCO_3}}\right)^{0.57} = 0.866 \quad (5)$$

$$K_d = 4.1\left(\frac{K_{FeCO_3}}{K_{SrCO_3}}\right)^{1.0} = 0.269 \quad (6)$$

where K_{FeCo_3} and K_{SrCO_3} are the solubility products for siderite and strontianite ($10^{-10.45}$ and $10^{-9.27}$, respectively; values from Stumm and Morgan, 1996). Note that because of solution boundary-layer-related effects, elements such as Sr with K_d values less than 1 are expected to yield experimental K_d' values that are greater than the theoretical K_d (Rimstidt et al., 1998). The mean experimental $D_{D\text{-}H}$ values obtained for Sr incorporation into abiotically precipitated $FeCO_3$(s) (Fig. 7B; see also Fig. 8) were substantially lower than calculated K_d' value, but bracketed the calculated K_d value. In contrast to these results, the mean $D_{D\text{-}H}$ value for Sr partitioning into siderite formed during HFO reduction in Ca-free systems (Fig. 6A) was five-fold higher than the predicted K_d and 1.5-fold higher than the predicted K_d'.

The high degree of Sr partitioning into biogenic siderite is surprising because the relatively large ionic radius (sixfold coordination; Shannon, 1976) of Sr^{2+} (1.18 Å) compared with Fe^{2+} (0.78 Å) would be expected to prevent major isomorphic substitution of Sr into the $FeCO_3$(s) lattice (Reeder, 1990). Rates of mineral precipitation strongly influence the degree of trace element partitioning into a major element precipitate (Morse and Mackenzie, 1990; Mucci and Morse, 1990) and the rapid rate of siderite precipitation during the latter stages of HFO reduction could perhaps be expected to account for the relatively high $D_{D\text{-}H}$ values obtained from the analysis in Figure 6. However, rates of $FeCO_3$(s) precipitation in the abiotic coprecipitation experiments containing 5 to 20 mM

$FeCl_2$ were equal to or greater than those occurring in the HFO reduction experiments (compare Fig. 7A with Fig. 1A). Thus, elevated rates of $FeCO_3$(s) precipitation cannot alone account for the anomalously high $D_{D\text{-}H}$ values for Sr partitioning into $FeCO_3$(s) observed in the HFO reduction experiments. It is important to note that, with the possible exception of phosphate (see below), the additional components present in the culture medium would have been expected to retard coprecipitation of Sr with $FeCO_3$(s) relative that occurring in their absence in the abiotic coprecipitation experiments. For example, the additional ionic strength must have reduced the aqueous phase activity of Fe^{2+} and CO_3^{2-}, and the additional trace metals (Ca, Co, Cu, Mg, Mn, Ni) may have competed with Sr for incorporation into solid-phase Fe(II) compounds (see discussion of the Ca effect below). Hence, the large difference in the extent of Sr coprecipitation with siderite observed during the HFO reduction vs. abiotic coprecipitation experiments cannot be attributed to differences in medium composition in the two different reaction systems.

Association of Sr with the surface of rapidly growing siderite crystals (e.g., through sorption to sites with remnant ionic charge or substitution at vacant surface lattice positions resulting from defects in crystal structure; Veizer, 1990) and subsequent entrapment of Sr within the siderite lattice provides a plausible explanation for the intensive scavenging of Sr during biologically induced siderite precipitation observed in this study. The capacity for carbonate minerals (e.g., calcite, siderite) surfaces to sorb divalent metal cations is well recognized (Morse, 1986; Wersin et al., 1989; Zachara et al., 1991), and the phenomenon of surface enrichment leading to trace element entrapment during crystal growth is widespread in natural systems (Watson, 1996). Surface enrichment and entrapment leads to preservation of a condition of thermodynamic disequilibrium relative to the equilibrium solid-solution composition of crystal phases (Watson, 1996). This process can account for the much higher functional partition coefficient for Sr incorporation into biogenic siderite compared with that expected from solid-solution theory. In addition, a zone of locally elevated pH and alkalinity (i.e., reduced H^+ activity) is likely to occur in the vicinity of the bacteria-oxide interface during Fe(III) oxide reduction (Roden and Edmonds, 1997; Zachara et al., 2002). By analogy to the influence of pH on trace metal sorption by calcite (Zachara et al., 1991), the presence of such a microenvironment may enhance the association of Sr^{2+} with reactive sites on the siderite surface, thereby promoting Sr surface enrichment and entrapment during crystal growth. This phenomenon may have contributed to the substantially higher $D_{D\text{-}H}$ values for Sr partitioning into biogenic vs. abiotically precipitated $FeCO_3$(s).

4.2.3. Coprecipitation with Noncarbonate Fe(II) Solids

Another potential explanation for the high $D_{D\text{-}H}$ values for Sr partitioning into biogenic Fe(II)(s) compounds is related to the apparent formation of substantial quantities of noncarbonate Fe(II)(s) during HFO reduction. It is possible that some of portion of the immobilized Sr coprecipitated with vivianite, which is likely to have formed through reaction of biogenic Fe(II) with PO_4^{3-} present in the culture medium (Fredrickson et al., 1998). Zachara et al. (2001) demonstrated incorporation of Co^{2+} into abiotically precipitated vivianite, and suggested that coprecipitation of Co^{2+} with biogenic vivianite may have influenced the extent of Co release to solution during bacterial reductive dissolution of Co-substituted goethite. However, it is unlikely that this process could have been responsible for the loss of Sr from solution observed during the latter stages of the Ca-free HFO reduction experiments reported here (Fig. 1B). Fredrickson et al. (1998) demonstrated near-complete removal of phosphate from solution during the first few days of HFO reduction by *S. putrefaciens* CN32 in $NaHCO_3$-buffered culture medium very similar to that employed in this study. Rapid and extensive precipitation of vivianite during HFO reduction is consistent with the very low solubility of this mineral (Al-Borno and Tomson, 1994), and the rapid kinetics of vivianite precipitation documented in other Fe(III) oxide reduction systems (Zachara et al., 1998). These considerations suggest that production of vivianite is likely to have occurred during the early stages of HFO reduction in our experiments—that is, at a time when Sr was being released to solution.

The possibility exists that Sr became associated with amorphous mixed Fe(II)-Fe(III) hydroxy compounds that were likely generated during HFO reduction. By analogy to amorphous HFO surfaces (Dzombak and Morel, 1990; Small et al., 1999), such phases would be expected to have substantial Sr^{2+} sorption capacity, particularly at the pH values observed in our experiments. Complexation of Sr by $Fe^{II}OH$ or $Fe^{III}OH$ surface sites could lead to surface enrichment and entrapment of Sr in a manner analogous to that suggested for siderite, thereby leading to enhanced Sr scavenging during the latter stages of HFO reduction. Incorporation of Sr into such phases provides an explanation for the apparent formation of noncarbonate solid-phase Sr during HFO reduction (Table 2), assuming such phases were subject to partial dissolution by the alkaline CD extraction procedure.

4.3. Influence of Ca on Sr Immobilization

In light of the propensity for coprecipitation of Sr with calcium carbonate minerals (Morse and Mackenzie, 1990; Mucci and Morse, 1990), we anticipated that the presence of mM levels of Ca in HFO reduction cultures would promote Sr immobilization through incorporation of Sr into $CaCO_3$(s) phases formed as a result of alkalinity generation during HFO reduction. In contrast to this expectation, the presence of 10 mM Ca strongly inhibited Sr incorporation into biogenic carbonate phases, despite the fact that wet-chemical (Figs. 2B,C) and XRD analyses (Figs. 5C) analyses suggested that large quantities (5 to 10 mmol L^{-1}) of $CaCO_3$(s) were produced. This result is clearly illustrated by the lack of correlation between solution-phase changes in Sr and Fe(II) in the 10 mM Ca systems (Fig. 6B, solid symbols).

Increases in pH (Figs. 1C, 2C) and SI values for strontianite (Figs. 3A,B) during HFO reduction were much smaller in Ca-amended than in Ca-free 1 mM Sr cultures. These results suggest that inhibition of Sr immobilization in Ca-amended 1 mM Sr cultures may have been caused at least in part by consumption of alkalinity and DIC during $CaCO_3$(s) precipitation. This mechanism does not apply, however, to the 100 μM and 10 μM Sr experiments, in which saturation with respect to strontianite was never achieved.

The ideas discussed in the preceding section provide the basis for an explanation of the negative influence of Ca on Sr scavenging during carbonate mineral precipitation in the 100 μM and 10 μM Sr HFO reduction systems. These arguments apply also to the 1 mM Sr cultures to the extent that coprecipitation with siderite (vs. strontianite formation) was responsible for Sr immobilization in these cultures. Calcium is known compete with Co (Kornicker et al., 1985) and Zn (Zachara et al., 1988) for sorption onto calcite surface sites. By analogy, it is logical to assume that Ca would compete with Sr for sorption onto siderite surfaces. Because surface complexation represents the first step in the process of solid solution formation (Stumm, 1992) as well as the general process of surface element and trace element uptake during heterogeneous crystal growth (Watson, 1996), the presence of a vast excess of Ca relative to Sr would be expected to inhibit (by a mass-action effect) coprecipitation of Sr with the $FeCO_3$(s) component of the ankerite produced in the Ca-amended HFO reduction cultures. This suggestion is supported by the observation by Mortimer and Coleman (1997) that high concentrations of Mg inhibited incorporation of Ca into siderite produced during bacterial HFO reduction.

To directly test the above assertion, we examined the influence of Ca on Sr partitioning into abiotically precipitated siderite. The results showed that 1 mM Ca strongly inhibited sequestration of 10 μM Sr during precipitation of ~10 mmol L^{-1} siderite (Fig. 8A). In this experiment, the $D_{D\text{-}H}$ value for Ca partitioning into siderite (0.252; Fig. 8B) was comparable to that observed for Sr partitioning into siderite in a parallel Ca-free system (0.190; Fig. 8B). These results are similar to those from Ca-amended vs. Ca-free HFO reduction experiments: the average $D_{D\text{-}H}$ value for Ca incorporation into siderite in Ca-amended cultures (0.800 $\pm$ 0.061; Fig. 6B) was comparable to that for Sr incorporation into siderite in Ca-free cultures (1.35 $\pm$ 0.13; Fig. 6A). These findings suggest that direct substitution of Ca for Sr took place at foreign element incorporation sites on growing crystal surfaces during both abiotic and microbially induced $FeCO_3$(s) precipitation. An analogous argument, so far untested, may explain the lack of Sr partitioning into the $CaCO_3$(s) component of ankerite produced in the Ca-amended HFO reduction cultures: the large quantity of Fe(II) generated during the initial stages of HFO reduction would be expected to compete with Sr for sorption on growing calcite surfaces, thereby blocking incorporation of Sr into the $CaCO_3$(s) lattice.

4.4. Biogeochemical Significance

The near-quantitative release of sorbed Sr during the initial stages of HFO reduction is consistent with previous field and laboratory studies documenting solubilization of trace and contaminant metals during dissimilatory microbial Fe(III) oxide reduction (Lovley, 1991, and references therein; Landa et al., 1991; Zachara et al., 2001). The observed immobilization of Sr during the latter stages of HFO reduction is a new finding, as it represents the first explicit demonstration of the sequestration of a contaminant metal through $FeCO_3$(s) formation coupled to microbial Fe(III) oxide reduction. A study of trace metal solubilization during microbial reduction of Co- and Ni-substituted goethite (Zachara et al., 2001) indicated that coprecipitation with siderite (and vivianite) may have contributed to retention of metals in the solid-phase during the oxide reduction process. However, in this study it was not possible to clearly distinguish between solid-phase sequestration of metals through adsorption/surface precipitation vs. authigenic mineral formation. Several articles have demonstrated sequestration of divalent metals in mixed Fe(II)-Fe(III) phases produced during bacterial reduction of HFO (Parmar et al., 2000; Fredrickson et al., 2001) as well as lepidocrocite and goethite (Cooper et al., 2000) reduction. Collectively, these studies emphasize that the traditional view of bacterial Fe(III) oxide reduction as a phenomenon responsible for trace/contaminant metal mobilization in sedimentary environments may not be universally applicable.

The spatial and temporal interplay between metal mobilization during microbial reductive dissolution of Fe(III) oxides and immobilization through precipitation of carbonate minerals and other biogenic Fe(II) solids is likely to have a crucial impact on the behavior of Sr and other divalent cations in Fe-rich anaerobic sedimentary environments. Metals mobilized during Fe(III) oxide reduction at a given place and time may be subject to immobilization later in time or in a different region of sediment where conditions become favorable for carbonate mineral precipitation. Many subsurface sediments contain up to several weight percent of iron oxides, which represent abundant electron acceptors for anaerobic respiration (Lovley, 1991; Nealson and Saffarini, 1994). A survey of published data (Lovley and Phillips, 1987; Chapelle and Lovley, 1992; Heron et al., 1994a,b; Heron and Christensen, 1995; Swartz et al., 1997; Anderson et al., 1998) on subsurface Fe(III) oxide abundance revealed whole sediment Fe(III) concentrations ranging from 1 to ~500 μmol per cm^3 wet sediment, with an average value of 168 $\pm$ 150 μmol cm^{-3} (n = 10). Although not all of the Fe(III) measured in these studies was present as amorphous HFO (the most available form for microbial reduction), studies indicate that a substantial fraction of the crystalline Fe(III) oxide content of natural subsurface materials is available for microbial reduction (Roden and Zachara, 1996; Zachara et al., 1998).

Given the substantial whole sediment concentrations of Fe(III) oxide present in the subsurface environments, the potential clearly exists for generation of large amounts of Fe(II), IC, and alkalinity coupled to microbial Fe(III) oxide reduction. Production of these species is expected to create conditions favorable for carbonate mineral precipitation. Studies of aquifer systems impacted by hydrocarbon or municipal landfill leachate contamination have demonstrated the presence of aqueous geochemical conditions favorable for siderite and calcite precipitation in zones of Fe(III) oxide reduction (Amirbahman et al., 1998; Baedecker et al., 1992), as well as the existence of authigenic siderite and calcite phases in aquifer solids (Amirbahman et al., 1998; Baedecker et al., 1992). In addition, microbial Fe(III) oxide reduction appears to be the main source of alkalinity leading to the ongoing precipitation of calcite in fractured granitic bedrock (Pedersen and Ekendahl, 1990; Pedersen, 1996). Analyses of groundwater/trace element interactions in subsurface systems indicate that Sr (100 to 9000 ppm) and other metals are commonly incorporated into calcites in situ (Lanstrom and Tullborg, 1995). Pye (1984) found substantial amounts of Sr (200 to 400 ppm) associated with si-

derite-calcite concretions in salt marsh sediments, which were later shown to be formed through the activity of sulfate-reducing bacteria that possess the capacity for Fe(III) oxide reduction (Coleman et al., 1993). These findings, together with the direct demonstration of Sr capture during HFO reduction reported here, suggest that bacterial Fe(III) oxide reduction could contribute to the immobilization of Sr and other metals in carbonate-rich aquifer environments. A number of U.S. Department of Energy sites suffer from varying levels of groundwater ^{90}Sr contamination (from $\sim$5 to $>$ 200 μM Sr), notably Hanford (DOE, 1998), Idaho National Engineering Laboratory (Duncan, 1995), and Oak Ridge National Laboratory (Jago et al., 1996). At Hanford, the size of the subsurface ^{90}Sr plume within the 200 area plateau is 100 times that of the ^{137}Cs and ^{239}Pu plumes, and ^{90}Sr concentrations in groundwater at the 100 N area are in excess of the drinking water standard (DOE, 1998). Our results suggest that formation of siderite and other biogenic Fe(II) solid formation coupled to microbial Fe(III) oxide reduction could influence ^{90}Sr contamination in subsurface sediments at these sites.

A comprehensive survey of trace element partitioning into carbonate minerals Rimstidt et al (1998) concluded that removal of divalent cations from solution through coprecipitation with relatively insoluble carbonate phases like siderite was likely to be much less effective than with more soluble phases such as calcite and magnesite. Our findings suggest, however, the need for caution in predicting the potential for contaminant metal sequestration in biogenic siderite based on solubility product considerations, or on the results of abiotic coprecipitation experiments. As discussed above, unique surface chemical phenomena associated with bacterial Fe(III) oxide reduction may lead to dramatically increased partitioning of trace metals into siderite and other biogenic Fe(II) solids relative to that expected for equilibrium or near-equilibrium solid solution formation. Studies of Sr and other trace-contaminant metal immobilization coupled to natural Fe(III) oxide reduction in experimental systems that simulate the biogeochemical conditions in subsurface sediments are required to further evaluate the significance of these processes. Our results with Ca-amended cultures suggest that it will be important to consider the impact of dissolved Ca in groundwaters on divalent metal sequestration during carbonate mineral precipitation. In addition, evaluation of the potential for Ostwald ripening to expel trace metals from biogenic Fe(II) solid precipitates is required to assess the long-term stability of such coprecipitates in subsurface environments.

5. CONCLUSIONS

Near-quantitative solubilization of sorbed Sr was observed during the early stages of bacterial amorphous HFO reduction. Aqueous Sr was subsequently immobilized during the latter stages of HFO reduction in Ca-free systems through one or more of the following mechanisms: (1) strontianite precipitation (1 mM Sr systems); (2) coprecipitation of Sr with siderite; (3) coprecipitation of Sr with noncarbonate Fe(II) solid phases. Direct correlations between Fe(II)(aq) and Sr(aq) during Sr immobilization in 100 μM Sr and 10 μM Sr reaction systems, which remained undersaturated with respect to strontianite, suggested that coprecipitation of Sr with biogenic Fe(II) solids was active. The average heterogeneous partition coefficient for Sr immobilization computed with Fe(II)(aq) and Sr(aq) data from these experiments was approximately fivefold in excess of values obtained during abiotic siderite precipitation experiments, as well as a theoretical $Fe(Sr)CO_3$ solid solution partition coefficient calculated by using the framework presented in Rimstidt et al. (1998). The high partition coefficients obtained in these experiments can be attributed to surface complexation and entrapment of Sr by rapidly growing siderite crystals and possibly other biogenic Fe(II) solids. These findings suggest the need for caution in predicting the potential for contaminant metal sequestration in biogenic siderite based on solubility product considerations or on the results of abiotic coprecipitation experiments. Unique surface chemical phenomena associated with bacterial Fe(III) oxide reduction may lead to dramatically increased partitioning of trace metals into siderite and other biogenic Fe(II) solids relative to that expected from equilibrium or near-equilibrium solid solution formation. These same surface phenomena are also likely responsible for the observed inhibition by Ca of Sr partitioning into biogenic Fe(II) solids, which (on the basis of the results of abiotic precipitation experiments) can be attributed to competition between Ca and Sr for surface complexation and entrapment by growing siderite crystals. The inhibition by Ca of Sr immobilization emphasizes the need for careful consideration of the influence of competing cations on the fate of trace metals in carbonate-bearing sediments. The spatial and temporal interplay between the Sr mobilization and immobilization processes associated with bacterial HFO reduction observed in this study is likely to have crucial impact on the behavior of Sr and other divalent cations in Fe-rich anaerobic sedimentary environments. Metals mobilized during Fe(III) oxide reduction at a given place and time may be subject to immobilization later in time or in a different region of sediment where conditions are favorable for siderite or other biogenic Fe(II)(s) mineral precipitation.

Acknowledgments—We thank Jolanta Nunley for assistance with the SEM and EDS analysis; Betsy Graham and Jim Donahoe for assistance with ICP and XRD analyses, respectively; and Joe Benson for advice on interpretation of XRD data. Thanks also to J. Morse, A. Mucci, and J. Zachara for advice on interpretation of trace metal coprecipitation data and to J. Fredrickson for review of an early version of the manuscript. The comments of three anonymous reviewers led to significant improvement. This research was supported by grants DE-FG07-96ER62317 and DE-FG07-96ER62321 from the U.S. Department of Energy, Office of Energy Research, Environmental Management Science Program.

Associate editor: D. E. Canfield

REFERENCES

Al-Borno A. and Tomson M. B. (1994) The temperature dependence of the solubility product constant of vivianite. *Geochim. Cosmochim. Acta* **58,** 5373–5378.

Aller R. C., Mackin J. E., and Cox R. T. J. (1986) Diagenesis of Fe and S in Amazon inner shelf muds: Apparent dominance of Fe reduction and implications for the genesis of ironstones. *Cont. Shelf Res.* **6,** 262–289.

Amirbahman A., Schonenberger R., Johnson C. A., and Sigg L. (1998) Aqueous- and solid-phase biogeochemistry of a calcareous aquifer system downgradient from a municipal solid waste landfill (Winterthur, Switzerland). *Environ. Sci. Technol.* **32,** 1933–1940.

Anderson R. T., Rooney-Varga J. N., Gaw C. V., and Lovley D. R. (1998) Anaerobic benzene oxidation in the Fe(III) reduction zone of

petroleum-contaminated aquifers. *Environ. Sci. Technol.* **32,** 1222–1229.

Baedecker M. J., Cozzarelli I. M., Evans J. R., and Hearn P. P. (1992) Authigenic mineral formation in aquifers rich in organic material. *7th International Symposium on Water–Rock Interaction: Proceedings* In: (eds. Y. K. Kharaka and A. S. Maest), 257–261. Balkema.

Bruno J., Wersin P., and Stumm W. (1992) On the influence of carbonate in mineral dissolution: II. The solubility of $FeCO_3$(s) at 25 degrees C and 1 atm pressure. *Geochim. Cosmochim. Acta* **56,** 1149–1155.

Chapelle F. H. and Lovley D. R. (1992) Competitive exclusion of sulfate reduction by Fe(III)-reducing bacteria: A mechanism for producing discrete zones of high-iron ground water. *Ground Water* **30,** 29–36.

Coleman M. L. (1993) Microbial processes: Controls on the shape and composition of carbonate concretions. *Mar. Geol.* **113,** 127–140.

Coleman M. L., Hedrick D. B., Lovley D. R., White D. C., and Pye K. (1993) Reduction of Fe(III) in sediments by sulphate-reducing bacteria. *Nature* **361,** 436–438.

Cooper D. C., Picardal F., Rivera J., and Talbot C. (2000) Zinc immobilization and magnetite formation via ferric oxide reduction by Shewanella putrefaciens 200. *Environ. Sci. Technol.* **34,** 100–106.

Davis J. A., Kent D. B., Rea B. A., Maest A. S., and Garabedian S. P. (1993) Influence of redox environment and aqueous speciation on metal transport in groundwater. *Metals in Groundwater* In: (eds. H. E. Allen, E. M. Perdue, and D. S. Brown), 223–273. Lewis Publishers.

DOE (1998) *Management and Integration of Hanford site*. GW/VZ activities. U.S. Department of Energy.

Doerner H. A. and Hoskins W. M. (1925) Co-precipitation of radium and barium sulfates. *J. Am. Chem. Soc.* **47,** 662–675.

Duncan P. R. (1995) *An Evaluation of the Potential for Remediating Hazardous Metals and Radionuclides in Aquifers and the Subsurface: A Summary Report*. Idaho National Engineering Laboratory, Biotechnology Group.

Dzombak D. A. and Morel F. M. M. (1990) *Surface Complexation Modeling: Hydrous Ferric Oxide*. Wiley.

Fish W. (1993) Sub-surface redox chemistry: A comparison of equilibrium and reaction-based approaches. *Metals in Groundwater* In: (eds. H. E. Allen, E. M. Perdue, and D. S. Brown), 73–101. Lewis Publishers.

Fredrickson J. K., Zachara J. M., Kennedy D. W., Dong H., Onstott T. C., Hinman N. W., and Li S. (1998) Biogenic iron mineralization accompanying the dissimilatory reduction of hydrous ferric oxide by a groundwater bacterium. *Geochim. Cosmochim. Acta* **62,** 3239–3257.

Fredrickson J. K., Zachara J. M., Kukkadapu R. K., Gorby Y. A., Smith S. C., and Brown C. F. (2001) Biotransformation of. Ni-substituted hydrous ferric oxide by an Fe(III)-reducing bacterium. *Environ. Sci. Technol.* **35,** 703–712.

Gautier D. L. (1982) Siderite concretions: Indicators of early diagenesis in the gammon shale (cretaceous). *J. Sed. Petrol.* **52,** 0859–0871.

Genin J. M. R., Bourrie G., Trolard F., Abdelmoula M., Jaffrezic A., Refait P. H., Maitre V., Humbert B., and Herbillon A. (1998) Thermodynamic equilibria in aqueous suspensions of synthetic and natural Fe(II)-Fe(III) green rusts: Occurrences of the mineral in hydromorphic soils. *Environ. Sci. Technol.* **32,** 1058–1068.

Genin J. M. R., Refait P., Bourrie G., Abdelmoula M., and Trolard F. (2001) Structure and stability of the Fe(II)-Fe(III) green rust"fougerite" mineral and its potential for reducing pollutants in soil solutions. *Appl. Geochem.* **16,** 559–570.

Hansen H. C. B. (1989) Composition, stabilization, and light absorption of Fe(II)-Fe(III) hydroxycarbonate (green rust). *Clay Miner.* **24,** 663–669.

Heron G., Christensen T. H., and Tjell J. C. (1994a) Oxidation capacity of aquifer sediments. *Environ. Sci. Technol.* **28,** 153–158.

Heron G., Crouzet C., Bourg A. C. M., and Christensen T. H. (1994b) Speciation of Fe(II) and Fe(III) in contaminated aquifer sediments using chemical extraction techniques. *Environ. Sci. Technol.* **28,** 1698–1705.

Heron G. and Christensen T. H. (1995) Impact of sediment-bound iron on redox buffering in a landfill leachate polluted aquifer (Vejen, Denmark). *Environ. Sci. Technol.* **29,** 187–192.

Hunter K. S., Wang Y., and VanCappellen P. (1998) Kinetic modeling of microbially-driven redox chemistry of subsurface environments: Coupling transport, microbial metabolism and geochemistry. *J. Hydrol.* **209,** 53–80.

Jackson R. E. and Inch K. J. (1983) Partitioning of strontium-90 among aqueous and mineral species in a contaminated aquifer. *Environ. Sci. Technol.* **17,** 231–237.

Jago W. K., Loffman R. S., and Motley C. A. (1996) *Oak Ridge Reservation Annual Environmental Report for 1995*. Oak Ridge National Laboratory.

Kornicker W. A., Morse J. W., and Damascenos R. N. (1985) The chemistry of Co^{2+} interaction with calcite and aragonite surfaces. *Chem. Geol.* **53,** 229–236.

Korobova E., Ermakov A., and Linnik V. (1998) ^{137}Cs and ^{90}Sr mobility in soils and transfer in soil-plant systems in the Novozybkov district affected by the Chernobyl accident. *Appl. Geochem.* **13,** 803–814.

Landa E. R., Phillips E. J. P., and Lovley D. R. (1991) Release of 226Ra from uranium mill tailings by microbial Fe(III) reduction. *Appl. Geochem.* **6,** 647–652.

Lanstrom O. and Tullborg E.-L. (1995) *Interactions of Trace Elements with Fracture Filling Minerals from the Casp Hard Rock Laboratory* SKB Technical Report 95-13. Swedish Nuclear Fuel and Waste Management Company.

Lippman F. (1973) *Sedimentary Carbonate Minerals*. Springer-Verlag.

Lovley D. R. (1991) Dissimilatory Fe(III) and Mn(IV) reduction. *Microbiol. Rev.* **55,** 259–287.

Lovley D. R. and Phillips E. J. P. (1986) Organic matter mineralization with reduction of ferric iron in anaerobic sediments. *Appl. Environ. Microbiol.* **51,** 683–689.

Lovley D. R. and Phillips E. J. P. (1987) Rapid assay for microbially reducible ferric iron in aquatic sediments. *Appl. Environ. Microbiol.* **53,** 1536–1540.

Lovley D. R., Stolz J. F., Nord G. L., and Phillips E. J. P. (1987) Anaerobic production of magnetite by a dissimilatory iron-reducing microorganism. *Nature* **330,** 252–254.

Lovley D. R. and Chapelle F. H. (1995) Deep subsurface microbial processes. *Rev. Geophys.* **33,** 365–381.

McIntire W. (1963) Trace element partition coefficients— A review of theory and applications to geology. *Geochim. Cosmochim. Acta* **27,** 1209–1264.

Mckinley J. P., Stevens T. O., Fredrickson J. K., Zachara J. M., Colwell F. S., Wagnon K. B., Smith S. C., Rawson S. A., and Bjornstad B. N. (1997) Biogeochemistry of anaerobic lacustrine and paleosol sediments within an aerobic unconfined aquifer. *Geomicrobiol. J.* **14,** 23–39.

Mehra O. P. and Jackson M. L. (1958) Iron oxide removal from soils and clays by a dithionite-citrate system buffered with sodium bicarbonate. *Clays Clay Min.* **7,** 317–327.

Morse J. W. (1986) The surface chemistry of calcium carbonate minerals in natural waters: An overview. *Mar. Chem.* **20,** 91–112.

Morse J. W. and Bender M. L. (1990) Partition coefficients in calcite: Examination of factors influencing the validity of experimental results and their application to natural systems. *Chem. Geol.* **82,** 265–277.

Morse J. W. and Mackenzie F. T. (1990) *Geochemistry of Sedimentary Carbonates*. Elsevier.

Mortimer R. J. G. and Coleman M. L. (1997) Microbial influence on the oxygen isotopic composition of diagenetic siderite. *Geochim. Cosmochim. Acta* **61,** 1705–1711.

Mortimer R. J. G., Coleman M. L., and Rae J. E. (1997) Effect of bacteria on the elemental composition of early diagenetic siderite: Implications for palaeoenvironmental interpretations. *Sedimentology* **44,** 759–765.

Mozley P. S. and Carothers W. W. (1992) Elemental and isotopic composition of siderite in the kuparuk formation, Alaska: Effect of microbial activity and water/sediment interaction on early porewater chemistry. *J. Sed. Petrol.* **62,** 681–692.

Mucci A. and Morse J. W. (1990) Chemistry of low-temperature abiotic calcites: Experimental studies on coprecipitation, stability, and fractionation. *Aquat. Sci.* **3,** 217–257.

Nealson K. H. and Saffarini D. (1994) Iron and manganese in anaerobic respiration: Environmental significance, physiology, and regulation. *Annu. Rev. Microbiol.* **48,** 311–343.

Nordstrom D. K., Plummer L. N., Langmuir D., Busenberg E., and May H. M. (1990) Revised chemical equilibrium data for major water-mineral reactions and their limitations. *Chemical Modeling of Aqueous Systems II* In: (eds. D. C. Melchior and R. L. Bassett), 398–413. Am. Chem. Soc..

Olsen C. R., Lowery P. D., Lee S. Y., Larsen I. L., and Cutshall N. H. (1986) Geochemical and environmental processes affecting radionuclide migration from a formerly used seepage trench. *Geochim. Cosmochim. Acta* **50,** 593–607.

Ona-Nguema G., Abdelmoula M., Jorand F., Benali O., Gehin A., Block J. C., and Genin J. M. R. (2002) Iron(II,III) hydroxycarbonate green rust formation and stabilization from lepidocrocite bioreduction. *Environ. Sci. Technol.* **36,** 16–20.

Parmar N., Warren L. A., Roden E. E., and Ferris F. G. (2000) Solid phase capture of strontium by the iron reducing bacteria Shewanella alga strain BrY. *Chem. Geol.* **169,** 281–288.

Parmar N., Gorby Y. A., Beveridge T. J., and Ferris F. G. (2001) Formation of green rust and immobilization of nickel in response to bacterial reduction of hydrous ferric oxide. *Geomicrobiol. J.* **18,** 375–385.

Pedersen K. (1996) Investigations of subterranean bacteria in deep crystalline bedrock and their importance for the disposal of nuclear waste. *Can. J. Microbiol.* **42,** 382–391.

Pedersen K. and Ekendahl S. (1990) Distribution and activity of bacteria in deep granitic groundwaters of southeastern Sweden. *Microb. Ecol.* **20,** 37–52.

Postma D. (1977) The occurrence and chemical composition of recent Fe-rich mixed carbonates in a river bog. *J. Sed. Petrol.* **47,** 1089–1098.

Postma D. (1981) Formation of siderite and vivianite and the pore-water composition of a recent bog sediment in Denmark. *Chem. Geol.* **31,** 225–244.

Postma D. (1982) Pyrite and siderite formation in brackish and freshwater swamp sediments. *Am. J. Sci.* **282,** 1151–1183.

Pye K. (1984) SEM analysis of siderite cements in intertidal marsh sediments, Norfold, England. *Mar. Geol.* **56,** 1–12.

Reeder R. J. (1990) Crystal chemistry of the rhombohedral carbonates. *Carbonates: Mineralogy and Chemistry*,, Vol. 11 In: (ed. R. J. Reeder), 1–48. Mineralogical Society of America.

Riley R. G., Zachara J. M., and Wobber F. J. (1992) *Chemical Contaminants on DOE Lands and Selection of Contaminant Mixtures for Subsurface Science Research*. U.S. Department of Energy.

Rimstidt J. D., Balog A., and Webb J. (1998) Distribution of trace elements between carbonate minerals and aqueous solutions. *Geochim. Cosmochim. Acta* **62,** 1851–1863.

Roden E. E. and Lovley D. R. (1993a) Dissimilatory Fe(III) reduction by the marine microorganism. *Desulfuromonas acetoxidans. Appl. Environ. Microbiol.* **59,** 734–742.

Roden E. E. and Lovley D. R. (1993b) Evaluation of ^{55}Fe as a tracer of Fe(III) reduction in aquatic sediments. *Geomicrobiol. J.* **11,** 49–56.

Roden E. E. and Zachara J. M. (1996) Microbial reduction of crystalline iron(III) oxides: Influence of oxide surface area and potential for cell growth. *Environ. Sci. Technol.* **30,** 1618–1628.

Roden E. E. and Edmonds J. W. (1997) Phosphate mobilization in iron-rich anaerobic sediments: Microbial Fe(III) oxide reduction versus iron-sulfide formation. *Arch. Hydrobiol.* **139,** 347–378.

Sahai N., Carroll S. A., Roberts S., and O'Day P. A. (2000) X-ray absorption spectroscopy of strontium(II) coordination. *J. Colloid. Interface Sci.* **222,** 198–212.

Salvage K. M. and Yeh G. T. (1998) Development and application of a numerical model of kinetic and equilibrium microbiological and geochemical reactions (BIOKEMOD). *J. Hydrol.* **209,** 27–52.

Saunders J. A. and Swann C. T. (1992) Nature and origin of authigenic rhodochrosite and siderite from the Paleozoic aquifer, northeast Mississippi, USA. *Appl. Geochem.* **7,** 375–387.

Schecher W. D. and McAvoy D. C. (1998) *MINEQL+: A Chemical Equilibrium Modeling System. Version 4.0 for Winders User's Manual*. Environmental Research Software.

Shannon R. D. (1976) Revised effective ionic radii and systematic studies of interatomic distances in halides and chalcogenides. *Acta Cryst.* **A32,** 751–767.

Small T. D., Warren L. A., Roden E. E., and Ferris F. G. (1999) Sorption of strontium by bacteria, Fe(II) oxide and bacteria-Fe(III) oxide composites. *Environ. Sci. Technol.* **33,** 4465–4470.

Smith R. M. and Martell A. E. (1997) *NIST Critically Selected Stability Constants of Metal Complexes Database: Version 3.0 User's Guide and Database Software.* NIST Standard Reference Database 46.

Sposito G. (1984) *The Surface Chemistry of Soils*. Oxford University Press.

Stumm W. (1992) *Chemistry of the Solid–Water Interface*. Wiley.

Stumm W. and Morgan J. J. (1996) *Aquatic Chemistry*. Wiley.

Swartz C. H., Ulery A. L., and Gschwend P. M. (1997) An AEM-TEM study of nanometer-scale mineral associations in an aquifer sand: Implications for colloid mobilization. *Geochim. Cosmochim. Acta* **61,** 707–718.

Tebes-Stevens C., Valocchi A. J., VanBriesen J. M., and Rittman B. E. (1998) Multicomponent transport with coupled geochemical and microbiological reactions: Model description and example simulations. *J. Hydrol.* **209,** 8–26.

Thornber M. R. and Nickel E. H. (1976) Supergene alterations of sulphides. III. The composition of associated carbonates. *Chem. Geol.* **17,** 45–72.

Trolard F., Genin J. M. R., Abdelmoula M., Bourrie G., Humbert B., and Herbillon A. (1997) Identification of a green rust mineral in a reductomorphic soil by Mossbauer and Raman spectroscopies. *Geochim. Cosmochim. Acta* **61,** 1107–1111.

Veizer J. (1990) Trace elements and isotopies in sedimentary carbonates. *Carbonates: Mineralogy and Chemistry,* 11 In: (ed. R. J. Reeder), 265–299. Mineralogical Society of America.

Watson E. B. (1996) Surface enrichment and trace-element uptake during crystal growth. *Geochim. Cosmochim. Acta* **60,** 5013–5020.

Wersin P., Charlet L., Karthein R., and Stumm W. (1989) From adsorption to precipitation: Sorption of Mn $^{2+}$ on $FeCO_3$(s). *Geochim. Cosmochim. Acta* **53,** 2787–2796.

Zachara J. M., Kittrick J. A., and Harsh J. B. (1988) The mechanism of Zn^{2+} adsorption on calcite. *Geochim. Cosmochim. Acta* **52,** 2281–2291.

Zachara J. M., Cowan C. E., and Resch C. T. (1991) Sorption of divalent metals on calcite. *Geochim. Cosmochim. Acta* **55,** 1549–1562.

Zachara J. M., Fredrickson J. K., Li S. W., Kennedy D. W., Smith S. C., and Gassman P. L. (1998) Bacterial reduction of crystalline Fe(III) oxides in single phase suspensions and subsurface materials. *Am. Mineral.* **83,** 1426–1443.

Zachara J. M., Fredrickson J. K., Smith S. C., and Gassman P. L. (2001) Solubilization of Fe(III) oxide-bound trace metals by a dissimilatory Fe(III) reducing bacterium. *Geochim. Cosmochim. Acta* **65,** 75–93.

Zachara J. M., Kukkadapu R. K., Fredrickson J. K., Gorby Y. A., and Smith S. C. (2002) Biomineralization of poorly crystalline Fe(III) oxides by dissimilatory metal reducing bacteria (DMRB). *Geomicrobiol. J.* **19,** 179–207.

Table A1. Total, aqueous, and carbonate-associated Sr in uninoculated culture medium without and with HFO (~40 mmol L^{-1}). Each value is from a single culture sampled 1, 2, or 7 d after Sr addition.

System	Sr addition	Time (d)	Total Sr[a]	Aqueous Sr[b]	Carbonate associated[c]
− HFO	1mM	1	1.033	1.027	ND[d]
		2	1.028	1.049	ND
		7	1.021	1.035	ND
	100 μM	1	110	111	ND
		2	111	112	ND
		7	109	110	ND
	10 μM	1	11.2	11.5	ND
		2	11.2	11.0	ND
		7	10.9	11.7	ND
+ HFO	1mM	1	0.991	0.507	ND
		2	1.022	0.429	0.001
		7	0.988	0.414	0.000
	100 μM	1	108	20.6	ND
		2	111	15.4	0.0
		7	104	16.0	0.0
	10 μM	1	10.7	0.7	ND
		2	10.4	0.5	0.0
		7	9.9	0.5	0.0

[a] Sr content of whole (unfiltered) culture samples (mmol L^{-1} for lmMSr system; otherwise μmol L^{-1}).

[b] Sr content of 0.2-λm-filtered culture samples (mM for lmMSr system; otherwise μM).

[c] From analysis of material retained by filtration after alkaline citrate–dithionite extraction (see Materials and Methods).

[d] Not determined.

Table A2. Aqueous Sr and Ca concentration and pH over time in uninoculated 1mM Sr cultures. Each value is the mean (range) of duplicate cultures.

System	Time (d)	Sr (mM)	Ca (mM)	pH
Ca free	0	0.505 (0.160)	ND[a]	7.02 (0.04)
	16	0.507 (0.010)		6.96 (0.02)
	34	0.509 (0.001)		7.03 (0.02)
10 mM Ca	0	0.696 (0.082)	7.19 (0.790)	6.77 (0.010)
	16	0.698 (0.000)	7.30 (0.020)	6.99 (0.010)
	34	0.708 (0.190)	7.41 (0.170)	7.00 (0.030)

[a] Not determined.